DOE/ET-53088-354 IFSR #354

# Theory of Weak Ion Temperature Gradient Driven Turbulence Near the Threshold of Instability

*N. Mattor*
Institute for Fusion Studies
The University of Texas at Austin
Austin, Texas 78712

*P. H. Diamond*
Department of Physics
University of California at San Diego
La Jolla, California 92093
and
General Atomics, Inc.
San Diego, California 92138

December 1988

# Theory of Weak Ion Temperature Gradient Driven Turbulence Near the Threshold of Instability

*N. Mattor*
Institute for Fusion Studies
The University of Texas at Austin
Austin, Texas 78712

*P. H. Diamond*
Department of Physics
University of California, San Diego
La Jolla, California 92093
and
General Atomics, Inc.
San Diego, California 92138

## Abstract

This paper presents a theory of weak ion temperature gradient driven turbulence near the threshold of instability. The model considers kinetic ions and adiabatic electrons in a sheared slab geometry. Linear theory shows that for $\eta_{th} < \eta_i \lesssim \eta_{th} + (1+1/\tau)L_n/L_s$ (where $\eta_{th} = 0.95$ is the instability threshold and $L_n/L_s \ll 1$) then $\gamma \ll \omega$ and a weak turbulence theory applies. The nonlinear wave kinetic equation indicates that ion Compton scattering is the dominant nonlinear saturation process. The wave kinetic equation is reduced to a differential equation for the spectrum, from which it is shown that the energy scatters to the linearly stable low $k_y$ modes. The resulting spectrum of fluctuation levels (peaked about $k_\perp \rho_i \simeq 1$) is much lower than that suggested by naïve extrapolation from the strong turbulence regime. The resulting ion thermal conductivity is also extremely low, so that strong ion heating can be expected to drive the ion temperature gradient to a level where this weakly turbulent threshold regime is surpassed.

## I. Introduction

In recent years, ion temperature gradient driven turbulence[1] ("$\eta_i$ turbulence") has become a promising explanation for the anomalous ion heat loss observed in tokamaks.[2] Most basically, the theory predicts that when the ion temperature gradient is steeper than some threshold value (parametrized by $\eta_i \equiv \frac{d \ln T_i}{d \ln n_0} > \eta_{th} \equiv 0.95$ in the simplest version of the theory[3]), the mode is destabilized and the resulting fluctuations cause ion heat conduction (parametrized by $\chi_i$). This feature can qualitatively explain such experimental results as the improved energy confinement ($\tau_E$) which accompanies pellet injection,[4] and the $\tau_E$ degradation that accompanies neutral beam heating of low confinement ("L-mode") plasmas.[5] Other successful qualitative predictions include the turbulent density fluctuations propagating in the ion drift direction observed in TEXT tokamak,[6] and also the equality of momentum and thermal confinement times for neutral beam heated tokamaks.[7,8,9] Quantitatively, strong turbulence theory predictions[1] of $\chi_i$ (valid in the "fluid limit" of $\eta_i \gg \eta_{th}$, where wave-particle interaction is negligible) are easily large enough to account for the anomalous heat loss observed.

With these strong indications of the relevance of the basic theory, the more detailed issue of self consistency arises. For the fluid regime, this requires that the predicted $\chi_i$ establishes an ion temperature profile consistent with the assumption that $\eta_i \gg \eta_{th}$. To examine this, a transport simulation has been performed,[10] which lets the profile evolve under the influence of the fluid regime $\chi_i$, combined with other sources and sinks of ion heat. The vanishing of $\chi_i$ at the instability threshold (not accounted for by the fluid regime formula) is modelled by interpolating between the fluid regime (for $\eta_i \gg \eta_{th}$) and 0 for $\eta_i \leq \eta_{th}$. Results show that this $\chi_i$ is large enough that the ion temperature gradient cannot steepen significantly above threshold, and remains well below the fluid regime level (even with strong ion heating present). However, the validity of using the fluid $\chi_i$ for the threshold region is by no means clear, since the character of the instability changes quite a bit as threshold is approached. Thus, in order to determine whether the regime of fluid theory is accessible, a separate theory is required to resolve the transport in the threshold regime.

Previous linear studies[3,11,12,13] have determined the location of the threshold analytically, and investigated the growth rate near threshold numerically, but very little analytical theory valid *near* the threshold has been developed. Construction of a rigorous linear theory of these modes is complicated by the facts that stability comes from ion Landau damping (requiring kinetic theory), and that near threshold the last unstable modes have $k_\perp \rho_i \simeq 1$ (leading to nonlocal interaction). The nonlinear and transport behaviour of the $\eta_i$ mode near the threshold has naturally been even less well understood. There have been mixing length estimates of the quasilinear $\chi_i$ near threshold,[14] but this approach leads to spurious results (such as a fluctuation level of $\tilde{\phi} \sim 1/k_\perp L$, which does not vanish at threshold). A reliable prediction requires more careful consideration.

The difference between the fluid and threshold regimes, in addition to linear Landau damping, involves several important changes in the nonlinear behaviour. First, as the growth rate becomes less than the frequency, the strong turbulence approximations of the fluid regime become invalid, and a transition to weak turbulence ensues. Commonly used estimates such as $e\tilde{\phi}/T \sim 1/k_\perp L$ to find saturation levels, and $D \sim \gamma/k_\perp^2$ for transport, apply only for strong turbulence, where the nonlinearities are large enough to balance the linear terms. For weak turbulence (where the nonlinearities are small), a calculation based on the wave kinetic equation is necessary to obtain reliable predictions. Second, the frequency broadening of strong turbulence becomes negligible, and the triad resonances that are automatically allowed in strong turbulence for matching wavevectors ($\vec{k} = \vec{k}' + \vec{k}''$) must satisfy the additional constraint of linear frequency matching ($\omega_{\vec{k}} = \omega_{\vec{k}'} + \omega_{\vec{k}''}$). Finally as linear wave particle resonances grow more important, nonlinear wave-particle interaction becomes a more effective saturation mechanism. A weak turbulence expansion is appropriate for considering these changes.

This paper presents a theory of $\eta_i$ transport near the threshold of instability, with an emphasis on weak turbulence theory. We consider the usual paradigm model of sheared slab geometry with gyrokinetic ions and adiabatic electrons. The linear theory uses an eigenmode analysis for the real part of the frequency (for $\gamma \simeq 0$), and a local approximation to find the growth rate. This technique retains the essential features and orderings of the threshold regime, but is also simple enough for construction of a tractable nonlinear theory. The nonlinear theory follows the weak turbulence expansion, whereby the linear modes are substituted iteratively into the nonlinearity (which is smaller by an approximate factor of $\gamma/\omega$). This leads to a wave kinetic equation, describing the evolution of the spectrum as a balance of linear growth and nonlinear scattering and damping. This is solved for the saturated spectrum, which is used to calculate the turbulent ion thermal flux.

The principal results of this paper are the following:

1. When $\eta_{th} \leq \eta_i < \eta_{th} + (1 + 1/\tau)\frac{L_n}{L_s}$, (where $\eta_{th} = 0.95$ and $L_n/L_s \ll 1$), then $\gamma \ll \omega$ and a weak turbulence expansion applies.
2. Linear theory shows that the unstable modes near threshold have frequency $\omega \sim (L_n/L_s)^2\omega_{*i}$, linear growth rate $\gamma \sim (L_n/L_s)(\eta_i - \eta_c)\omega_{*i}$, and width $\Delta_x \sim \rho_i$, where $\eta_c$ is the $k_\perp$ dependent threshold. Furthermore, only the $l = 0$ radial eigenmode mode is unstable at threshold.
3. The frequency is very dispersive, $\frac{d\ln\omega}{d\ln k_y} \neq 1$, and therefore wave-wave interactions and turbulent shielding are negligible in this regime.
4. Nonlinear saturation of the unstable modes occurs through ion Compton scattering to the lower $k_y$ modes, which are stable. The resulting spectrum is given by

$$\left(\frac{e\tilde{\phi}}{T_i}\right)^2 = \sqrt{\frac{2}{\pi}}\left(\frac{q\rho_i}{r\hat{s}}\right)\frac{(1+1/\tau)^2}{\eta_i^2}\left(\frac{L_n}{L_s}\right)^2\left(\frac{\rho_i}{L_s}\right)^2 I(b),$$

   where $I(b)$ is a spectral intensity function of $b = k_y^2\rho_i^2$, which vanishes at threshold and is concentrated about $b = 1$ (Fig. 2 and after Eq. (29)). The coefficient of $I(b)$ is smaller that that for $\eta_i \gg \eta_{th}$ by a factor on the order of $(L_n/L_s)^2 \ll 1$.
5. The ion thermal conductivity from turbulent $\vec{E} \times \vec{B}$ convection is given by

$$\chi_i = N_{th}\frac{(1+1/\tau)^2}{2\sqrt{\pi}}\left(\frac{L_T}{L_s}\right)^2\frac{\rho_i^2 v_i}{L_s}$$

   where $N_{th}$ is a threshold dependent function of $\eta_i$ given by Eq. (35) and shown in Figure 3. The magnitude of $\chi_i$ is less than an extrapolation from the $\eta_i \gg \eta_{th}$ regime by a factor on the order of $(L_T/L_s)^2 \ll 1$.

The remainder of this paper is organized as follows. Section II presents the basic model and equations used in the theory. Section III develops a simple semi-local linear theory (frequency, growth rate, and basic mode structure) valid in the neighborhood of the threshold. Section IV develops the nonlinear theory, including derivation of the wave kinetic equation, which is an integral equation for the spectrum. This equation is solved approximately for the saturated spectrum. Section V outlines the derivation of the ion thermal conductivity, $\chi_i$. Section VI contains a short summary and conclusions. Also of interest are Appendix A, which addresses the stability and growth of the $l > 0$ radial eigenmodes, and Appendix B, which addresses the stability of the flat density modes ($L_n/L_s \to \infty$).

## II. Basic Model

The goal of this work is to develop only the framework of an analytical theory of the $\eta_i$ instability near the threshold. The essential features of the $\eta_i$ instability are the drive from the ion temperature gradient, ion Landau damping (from magnetic shear) and the nonlinear $\vec{E} \times \vec{B}$ drift, which determines mode coupling and transport. These are described in our model by the nonlinear electrostatic ion gyrokinetic equation[15] with adiabatic electrons, in a sheared slab geometry, with all inhomogeneities (density, ion temperature, and magnetic shear) in the radial ($x$) direction.

In a sheared slab geometry, the magnetic field is given by $\vec{B} = B_0\,(\hat{z} + (x/L_s)\,\hat{y})$. There are density and ion temperature gradients in the $x$ direction, characterized by $L_n$ and $L_T$, where $-dn_0/dr = n_0/L_n$ and $-dT_i/dr = T_i/L_T$. In general, we consider the regime $L_T \sim L_n \ll L_s$, usually true for tokamaks. (We also consider, in Appendix B, the stability of the $L_n > L_s$ "flat density" case, which may be relevant to H-mode discharges.) Since all inhomogeneities are radial, then linear perturbations have the form $\tilde{f}\,(x) \exp(-i\omega t + ik_y y + ik_z z)$. The modes are centered about the point where $\vec{k} \cdot \vec{B} = 0$, which in the closed field line configuration of the tokamak is allowable only on rational surfaces, $x_s(\vec{k})$. The point $x = 0$ is chosen at the rational surface of the "test mode", so that $k_\parallel = k_y x/L_s$, and for the "background modes" (which are nonlinearly coupled to the test mode) $k_\parallel{}' = k_y{}'(x - x_s(\vec{k}'))/L_s \equiv k_y' x'/L_s$. The mode has low frequency, $\omega \lesssim \omega_{*i}$, radial width on the order of $\rho_i$ (since the broader modes are stabilized by Landau damping), and has phase velocity $\omega/k_\parallel \lesssim v_i$ over most of the mode.

In the gyrokinetic model, electrostatic ion dynamics are described by the phase space distribution function $F(\vec{r}, \vec{v}, t) = F_0(x, \vec{v}) + \tilde{f}(\vec{r}, \vec{v}, t)$, where $F_0$ is a local maxwellian (*i.e.*, with $n_0(x)$ and $T_i(x)$), and $\tilde{f}$ is the rapidly varying part of the distribution function. The nonadiabatic part of $\tilde{f}$ evolves according to the nonlinear gyrokinetic equation[15] in the electrostatic limit:

$$\left(\frac{\partial}{\partial t} + ik_{\|}v_{\|}\right)\tilde{h}_{\vec{k}} - \left(\frac{\partial}{\partial t} + i\omega_{*i}\left(1 + \eta_i\left(\frac{mv^2}{2T_i} - \frac{3}{2}\right)\right)\right)F_0 J_0\left(\frac{k_\perp v_\perp}{\Omega_i}\right)\frac{e\tilde{\phi}_{\vec{k}}}{T_i} =$$
$$\frac{e}{m_i\Omega_i}\sum_{\vec{k}'+\vec{k}''=\vec{k}} \hat{b}\cdot\left(\vec{k}' \times \vec{k}''\right) J_0\left(\frac{k_\perp{}' v_\perp}{\Omega_i}\right)\tilde{\phi}_{\vec{k}'}\tilde{h}_{\vec{k}''}, \tag{1}$$

where,

$$\omega_{*i} = \frac{cT_i}{eB}\frac{d\ln n_0}{dx}, \qquad \eta_i = \frac{d\ln T_i}{d\ln n_0}, \qquad F_0 = n_0\left(\frac{m}{2\pi T_i}\right)^{3/2} e^{-mv^2/2T_i}, \qquad \Omega_i = \frac{eB}{m_i c},$$

$J_0$ is the zeroth Bessel function, and $\|$ and $\perp$ refer to the magnetic field direction, $\hat{b} = \vec{B}/|B|$. The right hand side of this equation describes mode coupling due to the $\vec{E} \times \vec{B}$ nonlinearity.

Electrons are taken as adiabatic ($\tilde{n}_e = n_0 e\tilde{\phi}/T_e$), and Eq. (1) is closed with the quasineutrality equation, $\tilde{n}_e = \tilde{n}_i$, or

$$(1 + 1/\tau)\, n_0 \frac{e\tilde{\phi}_{\vec{k}}}{T_i} = \int d^3v\, J_0\left(\frac{k_\perp v_\perp}{\Omega_i}\right)\tilde{h}_{\vec{k}}, \tag{2}$$

where $\tau = T_e/T_i$.

Equations (1) and (2) describe the $\eta_i$ instability in both the fluid ($\eta_i \gg 1$) and kinetic ($\eta_i \sim 1$) regimes. The fluid equations that describe the $\eta_i$ instability are reproduced by the velocity moments of Eq. (1), in the $\omega/k_{\|} > v_i$ limit. Close to marginal stability, Landau damping becomes important ($\omega/k_{\|} > v_i$) and a weak turbulence expansion is applicable (valid in the $\gamma \ll \omega$ regime[17]). The latter is the limit examined in the remainder of this paper.

## III. Linear Theory

The focus of this paper is nonlinear dynamics and transport, so what we require from the linear theory is a simple model that describes the most basic properties of the frequency, growth rate, and structure of the modes. Several authors have discussed the linear behaviour of the $\eta_i$ mode near threshold, but none completely enough for our purposes. Coppi *et al.*[18] derived an integral equation which reduces to a differential equation when $k_\perp^2 \rho_i^2 \ll 1$; near threshold, however, the dominant modes have $k_\perp^2 \rho_i^2 \simeq 1$, described by the fully nonlocal integral equation. The physical reason for this radially nonlocal interaction is that the mode is both narrow ($\Delta_x \sim \rho_i$) and slow ($\omega/\omega_{*i} \ll L_n/L_s \ll 1$). Thus, correlation across the width of the mode (on an ion transit time scale of $\Delta_x/v_i \sim \Omega_i^{-1}$), dominates decorrelation over this distance (which occurs, through shear, on the slower time scale of $\Delta_x/\Delta\left(\omega/k_\parallel\right) \gg \Omega_i^{-1}$), resulting in strong nonlocal interaction. However, such integral equations are notoriously difficult to solve, and so threshold behaviour is generally analyzed with a gyrokinetic equation, which lends itself to two routes of approximation. First, a local approximation[3,11,12] has the advantage of allowing simple algebraic solution for $\omega(\vec{k})$, however it does nothing to resolve the mode structure, which is important for the nonlinear theory. The second method is to expand to order $(k_x\rho_i)^2 = \rho_i^2 \frac{\partial^2}{\partial x^2}$, and solve the resulting differential equation either analytically (directly or with a WKB approximation) or with a shooting code.[13] While this method does resolve the mode structure, for the present case it becomes overly complicated when carried out to the order necessary to resolve the weak growth rate, and furthermore, since it relies on a $(k_x\rho_i)^2$ expansion for modes which have width $k_x\rho_i \simeq 1$, it is not clear that this complication leads to a more reliable result than the method described below.

The present analysis calculates for the lowest order mode structure and frequency (real part only, with $|\gamma| \ll |\omega|$) by an expansion in $(k_x\rho_i)^2$, and finds the growth rate using local theory. The growth rate of the modes is then calculated by summing the local growth of the individual parts of the mode, which corresponds mathematically to $\frac{\partial}{\partial t}\int |\tilde{\phi}_{\vec{k}}|^2 dx = \int \frac{\partial}{\partial t}|\tilde{\phi}_{\vec{k}}|^2 dx$. Associating the former with the mode growth rate, and the latter with the local growth rate, we obtain the formula:

$$\gamma_{\vec{k}} = \frac{\int_{-\infty}^{\infty} \gamma_{\vec{k}}\left(k_{\|}\right)\left|\tilde{\phi}_{\vec{k}}\right|^{2} dx}{\int_{-\infty}^{\infty}\left|\tilde{\phi}_{\vec{k}}\right|^{2} dx}. \tag{3}$$

This semi-local mode analysis offers a tractable formulation of the linear dynamics, consistent with the ordering of this regime. The main approximation is the neglect of detailed nonlocal effects, and it is doubtful that anything short of solving the full integral equation could account for these properly.

Linearizing Eq. (1), Fourier transforming in $t$, solving for $\tilde{h}$, and substituting into Eq. (2) produces the following mode equation:

$$\epsilon_{\vec{k}}\left(\omega_{\vec{k}} + i\gamma_{\vec{k}}\right)\tilde{\phi}_{\vec{k}} = 0, \tag{4}$$

where the linear dielectric function is given by:

$$\epsilon_{\vec{k}}(\omega) = 1 + 1/\tau - \frac{\omega_{*i}}{\omega}\eta_i\Gamma_0\zeta^2 + \frac{\omega_{*i}}{\omega}\left(\frac{\eta_i}{\eta_c} - 1 - \zeta^2\eta_i + \frac{\omega}{\omega_{*i}}\right)\Gamma_0\zeta Z(\zeta). \tag{5}$$

Here $Z$ is the plasma dispersion function, and

$$\zeta = \omega/\sqrt{2}v_i k_{\|}, \qquad v_i^2 = T_i/m_i, \qquad \Gamma_n = e^{-b_\perp} I_n\left(b_\perp\right), \qquad b_\perp = k_x^2\rho_i^2 + b,$$
$$b = k_y^2\rho_i^2, \qquad \rho_i = \tfrac{v_i}{\Omega_i}, \qquad \omega = \omega_{\vec{k}} + i\gamma_{\vec{k}},$$

$I_n$ is a modified Bessel function, and $\eta_c^{-1} \equiv \frac{1}{2} + b_\perp\left(1 - \frac{\Gamma_1}{\Gamma_0}\right)$ is the $k_\perp$ dependent critical value[3] of $\eta_i$. It is useful to note here that the ordering in the threshold regime, which can be verified *a posteriori*, is

$$\omega/\omega_{*i} \sim s^2, \quad \zeta \sim s, \quad \eta_i - \eta_c < s,$$

where $s = L_n/L_s \ll 1$ is used as a small parameter.

*A. Local Analysis*

In the local approximation, Eq. (4) is solved treating $k_x$ algebraicly. Assuming that $\left|\gamma_{\vec{k}}\right| \ll \left|\omega_{\vec{k}}\right|$, we can make the standard approximation $\epsilon_{\vec{k}}\left(\omega_{\vec{k}} + i\gamma_{\vec{k}}\right) = \epsilon'_{\vec{k}}\left(\omega_{\vec{k}}\right) + i\epsilon''_{\vec{k}}\left(\omega_{\vec{k}}\right) +$

$i\gamma_{\vec{k}}\partial\epsilon'_{\vec{k}}/\partial\omega_{\vec{k}}$ (where $\epsilon = \epsilon' + i\epsilon''$). With this, and noting that $\epsilon''_{\vec{k}}\left(\omega_{\vec{k}}\right)$ comes only from the resonant part of $Z\left(\zeta\right)$, Eq. (4) may be manipulated into the form:

$$\epsilon'_{\vec{k}}(\omega_{\vec{k}}) = p - \frac{\omega_{*i}}{\omega}\eta_i\zeta^2 + \epsilon''_{\vec{k}}\frac{ReZ}{ImZ} = 0, \tag{6}$$

and after some straightforward manipulation,

$$\epsilon''_{\vec{k}}(\omega_{\vec{k}}) = \frac{\omega_{*i}}{\omega}\left(\frac{\eta_i}{\eta_c} - 1 - \frac{p-1}{p}\eta_i\zeta^2\right)\frac{p\zeta ImZ\left(\zeta\right)}{p + \zeta ReZ\left(\zeta\right)}, \tag{7}$$

where $p \equiv \left(1 + 1/\tau\right)/\Gamma_0$.

Expanding $Z\left(\zeta\right)$ for $\zeta \ll 1$ (*i.e.*, strong ion resonance), then solving Eq. (6) yields

$$\begin{aligned} \omega_{\vec{k}}\left(k_\parallel\right) &= \frac{pv_i^2k_\parallel^2}{\omega_{*i}}\left(\frac{\eta_i}{2} + \frac{\eta_i}{\eta_c} - 1\right)^{-1} \\ &\simeq \frac{2pv_i^2k_\parallel^2}{\eta_i\omega_{*i}}, \end{aligned} \tag{8}$$

where the latter equality comes from the ordering $|\eta_i - \eta_c| < s$ (derived later in this section from the $|\gamma| \ll |\omega|$ requirement) . From the above, it is easy to show that $\partial\epsilon'/\partial\omega_{\vec{k}} \simeq -p/\omega_{\vec{k}}$ and $\zeta = \sqrt{2}pv_ik_\parallel/\eta_i\omega_{*i}$, and then using $\gamma = \frac{-\epsilon''}{\partial\epsilon'/\partial\omega}$, we obtain the local growth rate:

$$\gamma_{\vec{k}}\left(k_\parallel\right) = \sqrt{2\pi}\frac{v_i\left|k_\parallel\right|}{\eta_i}\left[\frac{\eta_i}{\eta_c} - 1 - \frac{2p\left(p-1\right)v_i^2}{\eta_i\omega_{*i}^2}k_\parallel^2\right]\exp\left[-2\left(\frac{pv_ik_\parallel}{\eta_i\omega_{*i}}\right)^2\right]. \tag{9}$$

Equations (8) and (9) agree well with the numerical solutions of Eqs. (4) and (5), treated locally.[11] We briefly review their analytical stability criterion, here exhibited in Eq. (9) by the terms in the first set of brackets, which determine the sign of $\gamma_{\vec{k}}\left(k_\parallel\right)$. Since the coefficient of $k_\parallel^2$ is positive, then if $\eta_i > \eta_c$, there is a band of $k_\parallel$ (centered about $k_\parallel = 0$) for which $\gamma_{\vec{k}}(k_\parallel) > 0$. This corresponds nonlocally to an unstable fluctuation centered on the mode rational surface, and stabilized on the edges by Landau damping. If $\eta_i \leq \eta_c$, then $\gamma_{\vec{k}}(k_\parallel) \leq 0$ for all $k_\parallel$, and no instability exists. Figure 1 shows $\eta_c\left(b\right)$. From this plot, it is clear that as $\eta_i$ decreases from the fluid regime, the low $k_\perp$ modes (broader in $x$, thus more heavily Landau damped) are stabilized. Threshold occurs when the last mode is stabilized, which occurs for $b_{th} \simeq 1$ and $\eta_c\left(b_{th}\right) \equiv \eta_{th} \simeq 0.95$.

*B. Mode Analysis*

The most straightforward way to examine the mode structure is to expand every $\Gamma_n(b_\perp)$ in Eq. (5) to order $k_x^2\rho_i^2$, and treat the resulting differential equation with a WKB approximation. However, this analysis is rather complicated, and defeats the purpose of finding a *simple* formulation of the linear theory. A method to circumvent this complication comes from the insight gained from local theory that the dominant imaginary terms in the mode equation balance on the average (*i.e.*, the terms which vary as $\gamma$ and as $\frac{\eta_i}{\eta_c(b_\perp)}-1$, with *all* of $b_\perp$, before any expansion). While radial variation of $k_x$ leads to *some* nonvanishing imaginary part of the potential function, shooting code analysis confirms that the effects of this may be neglected to lowest order. Furthermore, it is not clear that this complication leads to a more reliable result than the present method, for the $k_x\rho_i \simeq 1$ modes. In the spirit of a semi-local theory, we shall neglect the imaginary part of the mode equation entirely.

Keeping only the dominant (real) part of Eq. (5) with the ordering of the local theory, taking $k_\parallel = k_y x/L_s$, and expanding in $k_x$ yields:

$$\rho_i^2 \frac{d^2\tilde{\phi}_{\vec{k}}}{dx^2} + \frac{1}{1-\Gamma_1/\Gamma_0}\left(1 - \frac{ps^2\omega_{*i}}{\eta_i\omega_{\vec{k}}}\frac{x^2}{\rho_i^2}\right)\tilde{\phi}_{\vec{k}} = 0, \tag{10}$$

where $s = L_n/L_s$, and the argument of $\Gamma_n$ is $b$ $(= k_y^2\rho_i^2)$ instead of $b_\perp$ as before. This is a Weber's equation, and the general solution is given by the Hermite functions:

$$\tilde{\phi}_{\vec{k}} = H_l\left(x/\Delta_x\right)\exp\left[-x^2/2\Delta_x^2\right] \tag{11}$$

where $\Delta_x^2 = \eta_i\omega_{\vec{k}}/ps^2\omega_{*i}$. Combining this with the dispersion relation, we find:

$$\omega_{\vec{k}} = \omega_{*i}\frac{ps^2}{\eta_i}\frac{\Delta_x^2}{\rho_i^2}, \tag{12}$$

and

$$\frac{\Delta_x^2}{\rho_i^2} = (2l+1)^2\left(1 - \frac{\Gamma_1}{\Gamma_0}\right). \tag{13}$$

This we regard as the lowest order structure of the mode, and may be modified by outward propagation (from $\epsilon''$, ignored here) or other effects.

The growth of the $l = 0$ mode is calculated using Eq. (3) with $\gamma_{\bar{k}}(x)$ given by Eq. (9) (assuming $L_n/L_s \ll 1$), yielding

$$\gamma_{\bar{k}} = \sqrt{2}\omega_{*i}\frac{L_n}{L_s}\frac{\Delta_x}{\eta_i\rho_i}\left[\frac{\eta_i}{\eta_c} - 1 - \frac{2p(p-1)}{\eta_i}\left(\frac{L_n}{L_s}\right)^2\frac{\Delta_x^2}{\rho_i^2}\right]. \tag{14}$$

The stability and growth of the $l > 0$ modes is derived in Appendix A. The stability threshold in the $L_n/L_s \to \infty$ (flat density) regime is derived in Appendix B.

We now discuss the main features of the linear theory. First, it may seem surprising that $\Delta_x$ is independent of $L_s$, since $k_\parallel$ sets the radial scale. However, this is also true in the $\eta_i \gg 1$ fluid limit, where $\Delta_x$ is determined by shielding from the polarization drift, and apparently the present case is similar. Furthermore, Eq. (13) is consistent with the kinetic shooting code results of Ref. 16, which found that $\Delta_x$ depends primarily on $l$, and not $L_s/L_T$ or $\eta_i$. Second, the frequency of these modes, given by Eq. (12), is just the local frequency evaluated at the mode edge (where $k_\parallel = k_y\Delta_x/L_s$). Third, the instability threshold of the modes is essentially the same as that of the local theory, but with a small correction from the last term in the brackets of Eq. (14) ($\sim (L_n/L_s)^2$) coming from the fact that modes of finite width cover both unstable and stable regions at threshold. We shall ignore it for the $l = 0$ mode, but for the broader $l > 0$ modes this correction becomes larger, so that these modes are not unstable in the $\eta_i \simeq \eta_c$ regime considered here (Appendix A). Finally, in comparison with the $\eta_i \gg \eta_{th}$ and $\gamma \gg \omega$ fluid regime, the real part of the frequency remains on the same order of magnitude in both regimes, $\omega \sim s^2\omega_{*i}$ (the frequency in the fluid limit may be checked from the dispersion relation in, e.g., Ref. 1), while the growth rate changes from $\gamma \sim (1+\eta_i)s\omega_{*i}$ in the fluid regime to $\gamma \sim (\eta_i - \eta_c)s\omega_{*i}$ here. That the basic ordering is the same in both threshold and fluid regimes (except for the $\eta_i$ dependence) implies that this is in fact a continuation of the same root.

We have checked the analytical results with a shooting code, which retains all the imaginary parts of Eqs. (4) and (5) and expands in $k_x^2\rho_i^2$ (although this is not necessarily more reliable than the present analysis for the $k_x\rho_i \simeq 1$ regime). Results confirm that the mode is basically gaussian in structure with width as predicted, albeit a small degree of propagation past the turning points occurs, typically resulting in $\Delta_x \propto (L_s/L_n)^\alpha$ with

$\alpha \lesssim 1/4$. In view of this kind of uncertainty, in the remainder of the paper we shall take $\tilde{\phi} \sim e^{-x^2/2\Delta_x^2}$, (with $\Delta_x$ unspecified and possibly complex), to allow for the possibility of unresolved broadening through propagation. (The method of calculating normal mode frequency and growth rate allows for this uncertainty.) When quantitative estimates require a mode width, Eq. (13) will be used.

The exactness of this mode analysis is somewhat uncertain (since we have relied on an expansion for $k_x^2\rho_i^2 \ll 1$), but several qualitative features may be expected to persist in a more detailed solution. First, the turning points in Eq. (10) would be the same even without expansion in $k_x$, since at these points, $k_x \to 0$. The existence of these fixed turning points indicates that even in a more exact theory there will be a normal mode (as opposed to a convective mode) whose width is on the order of $\rho_i$ (*i.e.*, the separation of the turning points). Second, the radial quantization (parametrized by $l$) may be regarded as a real physical effect, since the modes are radial bound states. Finally, it is reasonable that only the $l = 0$ mode is unstable at the threshold, since the higher modes are broader, and hence more heavily Landau damped.

The validity of this theory depends on the $|\gamma| \ll |\omega|$ and $|\omega| \ll |k_\parallel v_i|$ assumptions. The former of these gives the strongest restriction. Either by comparing the $\gamma_{\vec{k}}$ and $\omega_{\vec{k}}$ of the normal mode, or by requiring in the local theory that the region where $\gamma(k_\parallel) > \omega(k_\parallel)$ (which will always occur at the mode center, since $\omega \propto k_\parallel^2$ while $\gamma \propto k_\parallel$ near the rational surface) occupy a negligible part of the mode, we obtain the restriction:

$$|\eta_i - \eta_c| < \frac{1 + 1/\tau}{\sqrt{2}\Gamma_0} \frac{\Delta_x}{\rho_i} \frac{L_n}{L_s} \simeq (1 + 1/\tau)\frac{L_n}{L_s}. \tag{15}$$

This range is plotted in Fig. 1. Since $L_n/L_s \ll 1$, Eq. (15) means that the range of $\eta_i$ covered by this theory is rather narrow. It appears that $|\omega| \ll |k_\parallel v_i|$ remains true well above this threshold regime, meaning that between the fluid and threshold regimes there exists a third regime, characterized by $\gamma \gtrsim \omega$ (invalidating the present expansion) and $|\omega| \ll |k_\parallel v_i|$ (ion resonances). This regime is discussed further in Section VI.

For a fixed value of $\eta_i$, Eq. (15) limits the range of validity in $k_y$ space. Letting $k_y = k_{y,crit} + \delta k_y$ (where $k_{y,crit}$ is the marginally stable $k_y$ for fixed $\eta_i$), then Eq. (15)

yields:

$$|\delta k| \lesssim \left(\sqrt{2}\frac{1+1/\tau}{\Gamma_0}\frac{L_n}{\eta_i L_s}\frac{\Delta_x}{\rho_i}\Big/\frac{\partial^2\eta_c}{\partial k_y^2}\right)^{1/2} \simeq k_{y,crit}\left(\frac{L_n}{L_s}\right)^{1/2}$$

In other words, as $k_y \to 0$ past $k_{y,crit} - \delta k$, the mode becomes *strongly* stabilized, so that $|\gamma| > |\omega|$ (Fig. 1). Hence these low $k_y$ modes are not described by our theory, but they are probably not important in the spectrum energy balance. This is discussed further in the next section.

Finally, we note that our theory seems to predict instability for the $k_y\rho_i \to \infty$ modes. However, this result is probably unphysical, since at shorter wavelength, certain stabilizing effects appear which are ignored in this theory, such as collisional viscosity or electron dissipation.

### IV. Nonlinear Theory

This section examines the transfer of fluctuation energy from unstable to stable linear modes, in order to determine the turbulent spectrum. The weak turbulence expansion is used to derive the wave kinetic equation, which is solved to yield the fluctuation level and spectrum at saturation.

The weak turbulence expansion[17] proceeds as follows. Noting that the linear part of Eq. (1) is of order $\omega\tilde{h}$, while the nonlinearity is of order $\gamma\tilde{h}$ (Eq. (21) verifies *a posteriori* that the saturation amplitude of the fluctuations is of order $\gamma$), then for $\gamma < \omega$ the equation can be solved by perturbing about the linear solution as follows. For simplicity of notation, we write Eq. (1) as

$$L_{1,\vec{k}}\tilde{h}_{\vec{k}} + L_{2,\vec{k}}\tilde{\phi}_{\vec{k}} = \sum_{\vec{k}'} C_{\vec{k}',\vec{k}''}\tilde{\phi}_{\vec{k}'}\tilde{h}_{\vec{k}''} \tag{16}$$

with $L_{1,\vec{k}}, L_{2,\vec{k}}$, and $C_{\vec{k}',\vec{k}''}$ defined from the corresponding terms in Eq. (1). Letting $\tilde{h}_{\vec{k}} = \tilde{h}^{(1)}_{\vec{k}} + \tilde{h}^{(2)}_{\vec{k}} + \ldots$, we have, to lowest order, the linear equation:

$$L_{1,\vec{k}}\tilde{h}^{(1)}_{\vec{k}} + L_{2,\vec{k}}\tilde{\phi}_{\vec{k}} = 0, \tag{17}$$

and to $n^{\text{th}}$ order,

$$L_{1,\vec{k}}\tilde{h}^{(n)}_{\vec{k}} = \sum_{\vec{k}'} C_{\vec{k}',\vec{k}''}\tilde{\phi}_{\vec{k}'}\tilde{h}^{(n-1)}_{\vec{k}''}. \tag{18}$$

Equations (17) and (18) are solved by iteratively substituting $\tilde{h}_{\vec{k}}^{(1)}$ into the nonlinearity of the second order equation, and repeating to $n^{\text{th}}$ order. Substituting $\tilde{h}_{\vec{k}}^{(1)}+\tilde{h}_{\vec{k}}^{(2)}+\tilde{h}_{\vec{k}}^{(3)}$ into Eq. (2) produces

$$\epsilon_{\vec{k}}^{(1)}(\omega)\,\tilde{\phi}_{\vec{k}}+\sum_{\substack{\vec{k}'+\vec{k}''=\vec{k}\\ \omega'+\omega''=\omega}}\epsilon^{(2)}_{\vec{k}',\vec{k}''}(\omega',\omega'')\tilde{\phi}_{\vec{k}'}\tilde{\phi}_{\vec{k}''}$$
$$+\sum\sum_{\substack{\vec{k}'+\vec{k}''+\vec{k}'''=\vec{k}\\ \omega'+\omega''+\omega'''=\omega}}\epsilon^{(3)}_{\vec{k}',\vec{k}'',\vec{k}'''}(\omega',\omega'',\omega''')\tilde{\phi}_{\vec{k}'}\tilde{\phi}_{\vec{k}''}\tilde{\phi}_{\vec{k}'''}=0 \tag{19}$$

where the symmetrized dielectric functions are given by

$$\epsilon_{\vec{k}}^{(1)}(\omega)=(1+1/\tau)\frac{n_0 e}{T_i}+\int d^3v\frac{J_0 L_{2,\vec{k}}}{L_{1,\vec{k}}}$$

$$\epsilon^{(2)}_{\vec{k}',\vec{k}''}(\omega',\omega'')=\frac{1}{2}\int d^3v\frac{J_0 L_{2,\vec{k}''}}{L_{1,\vec{k}'+\vec{k}''}L_{1,\vec{k}''}}C_{\vec{k}'\vec{k}''}\quad+\quad\left(\vec{k}'\leftrightarrow\vec{k}''\right)$$

$$\epsilon^{(3)}_{\vec{k}',\vec{k}'',\vec{k}'''}(\omega',\omega'',\omega''')=\frac{1}{2}\int d^3v\frac{J_0 L_{2,\vec{k}'''}}{L_{1,\vec{k}}L_{1,\vec{k}''+\vec{k}'''}L_{1,\vec{k}'''}}C_{\vec{k}',\vec{k}''+\vec{k}'''}C_{\vec{k}'',\vec{k}'''}$$
$$+\left(\vec{k}''\leftrightarrow\vec{k}'''\right),$$

where $J_0=J_0\left(\frac{k_\perp v_\perp}{\Omega_i}\right)$. Following Ref. 17, Eq. (19) may be divided into two equations. The real part becomes an equation for the frequency and linear structure of the mode,

$$\epsilon'_{\vec{k}}\left(\omega_{\vec{k}}\right)\tilde{\phi}_{\vec{k}}=0, \tag{20}$$

as examined in Section III. The imaginary part of Eq. (19), after some manipulation, becomes the wave kinetic equation, which describes linear instability and nonlinear evolution of the spectrum

$$\frac{1}{2}\frac{\partial\epsilon'}{\partial\omega_{\vec{k}}}\frac{\partial}{\partial t}\left|\tilde{\phi}_{\vec{k}}\right|^2=-\epsilon''_{\vec{k}}\left(\omega_{\vec{k}}\right)\left|\tilde{\phi}_{\vec{k}}\right|^2+Im\sum_{\substack{\vec{k}'+\vec{k}''=\vec{k}\\ \omega'+\omega''=\omega}}\frac{2\left|\epsilon^{(2)}_{\vec{k}',\vec{k}''}\left(\omega_{\vec{k}'},\omega_{\vec{k}''}\right)\right|^2}{\epsilon^{(1)}_{\vec{k}'+\vec{k}''}\left(\omega_{\vec{k}'}+\omega_{\vec{k}''}\right)}\left|\tilde{\phi}_{\vec{k}'}\right|^2\left|\tilde{\phi}_{\vec{k}''}\right|^2$$
$$+Im\sum_{\substack{\vec{k}'+\vec{k}''=\vec{k}\\ \omega'+\omega''=\omega}}\frac{4\epsilon^{(2)}_{\vec{k}',\vec{k}''}\left(\omega_{\vec{k}'},\omega_{\vec{k}''}\right)\epsilon^{(2)}_{\vec{k},-\vec{k}'}\left(\omega_{\vec{k}},-\omega_{\vec{k}'}\right)}{\epsilon^{(1)}_{\vec{k}''}\left(\omega_{\vec{k}''}\right)}\left|\tilde{\phi}_{\vec{k}'}\right|^2\left|\tilde{\phi}_{\vec{k}}\right|^2$$
$$-Im\sum_{\vec{k}'+\vec{k}''=\vec{k}}\epsilon^{(3)}_{\vec{k}',-\vec{k}',\vec{k}}\left(\omega_{\vec{k}'},-\omega_{\vec{k}'},\omega_{\vec{k}}\right)\left|\tilde{\phi}_{\vec{k}'}\right|^2\left|\tilde{\phi}_{\vec{k}}\right|^2, \tag{21}$$

where $\epsilon^{(1)}_{\vec{k}} = \epsilon'_{\vec{k}} + i\epsilon''_{\vec{k}}$, and $\omega_{\vec{k}}$ refers to only the real part of the frequency.

Physically, nonlinear transfer is the result of two processes. First are three-wave resonances, described by the second and third terms on the right hand side of Eq. (21). This is a transfer of energy between the test mode $\vec{k},\omega$ and background modes $\vec{k}',\omega'$ and $\vec{k}'',\omega''$, and requires a match of both wavenumber ($\vec{k} = \vec{k}'+\vec{k}''$) and frequency ($\omega = \omega'+\omega''$). Although this process dominates when $\eta_i \gg \eta_{th}$ (in strong turbulence[1]), in the present case it is much less important. This is because triads of waves which satisfy both $\vec{k}$ and $\omega_{\vec{k}}$ matching are rare, since $\omega_{\vec{k}}$, given by Eq. (12), is strongly dispersive ($\frac{d\ln\omega}{d\ln k_y} \neq 1$), and frequency broadening is negligible for weak turbulence ($\Delta\omega \simeq \gamma \ll \omega$). The second nonlinear coupling process is ion Compton scattering (also known as nonlinear Landau damping), described by the last term on the right hand side of Eq. (21). This is a transfer of energy between two modes $\vec{k},\omega$ and $\vec{k}',\omega'$ which occurs when an ion resonates with their beat wave, *i.e.* $v_{\|i} = (\omega - \omega')\,/(k_\| - k'_\|)$. Compton scattering dominates energy transfer in the threshold regime, accompanying the presence of significant *linear* wave-ion resonances.

Neglecting the three-wave resonance terms, (as well as turbulent shielding, for the same reason) we can write the wave kinetic equation as:

$$\frac{1}{2}\frac{\partial}{\partial t}\left|\phi_{\vec{k}}\right|^2 = \gamma^l_{\vec{k}}\left|\phi_{\vec{k}}\right|^2 + \gamma^c_{\vec{k}}\left|\phi_{\vec{k}}\right|^2, \tag{22}$$

where $\gamma^l_{\vec{k}}$ is the local linear growth rate, Eq. (9), and $\gamma^c_{\vec{k}}$ is the nonlinear Compton scattering term:

$$\begin{aligned}\gamma^c_{\vec{k}} =& \frac{\Omega_i^2}{\omega_{\vec{k}}^2} Im \sum_{\vec{k}'}\left\{\rho_i^4(\vec{k}\times\vec{k}')_\|^2 \int d^3v\, J_0^2 J_0'^2 \left(R_{\vec{k}'}\left(\omega_{\vec{k}'}\right) + R_{\vec{k}-\vec{k}'}\left(\omega_{\vec{k}} - \omega_{\vec{k}'}\right)\right)\left|\frac{e\tilde{\phi}_{\vec{k}'}}{T_i}\right|^2\right\} \\ &\div \frac{\partial\epsilon'_{\vec{k}}}{\partial\omega_{\vec{k}}},\end{aligned} \tag{23}$$

where,

$$J_0 = J_0\left(\frac{k_\perp v_\perp}{\Omega_i}\right), \qquad J_0' = J_0\left(\frac{k'_\perp v_\perp}{\Omega_i}\right),$$

$$R_{\vec{k}}(\omega) = -\frac{eF_0}{T_i}\ \frac{\omega - \omega_{*i}\left(1 + \eta_i\left(\frac{mv^2}{2T_i} - \frac{3}{2}\right)\right)}{\omega - k_\| v_\|}.$$

In deriving Eq. (23), the test mode has been assumed situated at $x = 0$, so that $k'_{\|} > k_{\|} \rightarrow 0$. None of the linear theory has been used in deriving Eq. (23).

Equation (22) suggests that a possible saturation mechanism for the linear instability is Compton scattering to the lower $k_y$ damped modes, which can dissipate energy. We now discuss several details of this mechanism. First, the tendency for Compton scattering to transfer energy to lower wavenumbers will be demonstrated from the form of $\gamma^c_{\vec{k}}$ after it has been further refined. Second, although we speak informally of Compton scattering only in terms of energy transfer between modes, this is not strictly the case. In the scattering process, some energy is lost to the scattering ion (in the form of nonlinear Landau damping), so that the true saturation mechanism is some combination of scattering and nonlinear damping. However, in either case, the ultimate sink of wave energy is heating of ions, leading to a net ion thermal diffusion as calculated in Section V. Third, Compton scattering is a binary process, and transfer from $\vec{k}$ to $\vec{k}'$ requires that the product $\tilde{\phi}_{\vec{k}}(x)\tilde{\phi}_{\vec{k}'}(x)$ be nonzero, which in turn requires finite levels of excitation for both modes (as well as mode overlap). The finite excitation level for linearly stable modes can be provided by nonlinear destabilization (*i.e.*, when $\gamma^l_{\vec{k}} + \gamma^c_{\vec{k}} > 0$), as described by Eq. (22). Finally, we note that that there must be enough modes to cover a given radial interval, *i.e.*, $\sum_{k'} \Delta'_x > \Delta r$. Estimating the mode width as $\rho_i$, and noting that the number of modes between $r$ and $r+\Delta r$ with poloidal modenumber $m$ is, on the average, $m/q(r) - m/q(r+\Delta r)$ (where $q$ is the safety factor and $\hat{s} = d\ln q / d\ln r$), we find the condition

$$m_{max} \gtrsim \sqrt{qr/\rho_i \hat{s}} \sim 30$$

(estimated for $r \sim 1\mathrm{m}$, $\rho_i \sim 1\mathrm{mm}$, and $q \sim \hat{s} \sim 1$). Typically this condition is easily met.

Several simplifications render Eq. (22) more tractable. First, we convert the discrete spectral sum (which involves complicated information about the rational surface of each mode) into an integral over the distribution of modes, with a density of states. Smoothing the mode distribution in $x'$ (to avoid rational surface information), and $k'_y$ (to avoid discrete $m$ information) results in

$$\sum_{k'_y} \longrightarrow \frac{r\hat{s}}{q} \int dk'_y \, |k'_y| \int dx'.$$

Second, it is useful to decompose the spectrum as

$$\left|\frac{e\tilde{\phi}_{\vec{k}'}}{T_i}\right|^2 = S\left(k'_y\right)\exp(-x'^2/\Delta_{x'}^2),$$

where $S(k_y)$ is the spectral amplitude and $\exp(-x'^2/\Delta_{x'}^2)$ accounts for the linear mode structure, Eq. (11). Finally, by averaging Eq. (22) over the width of the test mode (*i.e.*, in $x$), the local linear growth rate becomes the modal one (following the method of the linear theory), and the odd term of $(\vec{k}\times\vec{k}')_{\|}^2$ in $\gamma_{\vec{k}}^c$ vanishes from the antisymmetry of $k_x$ ($\sim x/\Delta_x^2$ for the $l=0$ mode). After some tedious algebra, this produces

$$\gamma_{\vec{k}}^c = -\sqrt{\frac{\pi}{2}}\frac{r\hat{s}}{q\rho_i}\frac{\Omega_i L_s \Gamma_0}{(1+1/\tau)\omega_{\vec{k}}}\int_{-\infty}^{\infty}\frac{dx'}{|x'|}\int_{-\infty}^{\infty}dk'_y K(k_y,k'_y)\exp\left(-\frac{x'^2}{\Delta_{x'}^2}\right)S\left(k'_y\right), \tag{24}$$

where the kernel of the integral is given by

$$\begin{aligned}K(k_y,k'_y) =& \rho_i^4\left(k_x^2 k'^2_y + k_y^2 k'^2_x\right)G\left(b,b'\right)\exp\left[-\frac{\left(\omega_{\vec{k}}-\omega_{\vec{k}'}\right)^2}{2s^2\omega'^2_{*i}}\frac{\rho_i^2}{x'^2}\right]\\ &\times\left\{\left(\omega_{*i}-\omega'_{*i}\right)\left[\left(\frac{1}{2}+\frac{G'\left(b,b'\right)}{G\left(b,b'\right)}\right)\eta_i - 1\right] - \left(\omega_{*i}-\omega'_{*i}\right)\frac{\eta_i}{2}\frac{\left(\omega_{\vec{k}}-\omega_{\vec{k}'}\right)^2}{s^2\omega'^2_{*i}}\frac{\rho_i^2}{x'^2}\right.\\ &\left.\quad + \omega_{\vec{k}} - \omega_{\vec{k}'}\right\}\end{aligned}$$

The contribution from $R_{\vec{k}'}$ in Eq. (23) has vanished from symmetry in $k'_y$ (*i.e.* $S\left(k'_y\right) = S\left(-k'_y\right)$, following from symmetry of the equations), and

$$G\left(b,b'\right) = \int_0^{\infty} d(v_\perp^2) J_0^2\left(\sqrt{2b}v_\perp\right) J_0^2\left(\sqrt{2b'}v_\perp\right) e^{-v_\perp^2},$$

$$G'\left(b,b'\right) = \frac{\partial}{\partial\alpha}G\left(\frac{b}{\alpha},\frac{b'}{\alpha}\right)\bigg|_{\alpha=1}.$$

With $\gamma_{\vec{k}}^c$ in the form of Eq. (24), the wave kinetic equation is an integral equation for $S(k_y)$. The integral operator in $\gamma_{\vec{k}}^c$ closely resembles that in the integral equation that formally describes the linear $\eta_i$ instability.[18] The primary difference is that the $x'$ integral in the present case, representing spatial overlap of different modes, is replaced with a time integral in the linear case, representing self interaction within one mode.

In both the linear and nonlinear cases, few methods are available for direct solution of the full integral equation. One numerical approach to the solution might be to let a test spectrum evolve via the wave kinetic equation, until a steady state spectrum is attained (which avoids the numerical instability associated with direct inversion of the integral operator). However, numerical solution is beyond the scope of the present work. Analytically, we are necessarily limited to rather approximate methods for finding $S(k_y)$. A simple but often reliable method (used in a previous version of this theory[19] and compared with the present version as a rough check) is to estimate of the integrated spectral amplitude in terms of the basic scalings and *rms* type quantities. An improvement over this method, which we now follow, is to Taylor expand $S(k_y')$ about $k_y \simeq k_y'$, which reduces the integral equation to a more tractable differential equation for $S(k_y)$.

Letting $k_y - k_y' = k_y''$, then

$$S(k_y') \simeq S(k_y) - k_y'' \frac{\partial S(k_y)}{\partial k_y} + \frac{k_y''^2}{2} \frac{\partial^2 S(k_y)}{\partial k_y^2}.$$

Since $S(k_y')$ in narrower than the kernel in $k_y'$-space, then extracting $S$ from the integration extends the domain over which the kernel is integrated. Therefore, it is necessary to accompany the extraction of $S$ with a normalization of the integral, as $\int_{-\infty}^{\infty} SKdk_y' \to S\int_{-\Delta_{SK}}^{\Delta_{SK}} Kdk_y' \simeq S\frac{\Delta_{SK}}{\Delta_K}\int_{-\infty}^{\infty} Kdk_y'$, where $S$ and $K$ represent the spectrum and kernel, respectively, and $\Delta_{SK}$ and $\Delta_K$ are the widths of $SK$ and $K$ in $k_y'$-space. While this step is heuristic, one can demonstrate that such a normalization factor is present for $S$ gaussian (Appendix C), and the results produced will be justified a *posteriori*. Also expanding other functions of $k_y'$ as $f(k_y') \simeq f(k_y) - k_y''\partial f/\partial k_y$ for $f = k_x', \omega_{k'}$, or $G(b, b')$, then $\gamma_{\vec{k}}^c$ becomes, for $k_y'' \ll k_y$,

$$\begin{aligned}\gamma_{\vec{k}}^c =& \sqrt{\frac{\pi}{2}} \frac{r\hat{s}}{q\rho_i} \frac{\Omega_i L_s \Gamma_0}{(1+1/\tau)\omega_{\vec{k}}} \frac{\Delta_{SK}}{\Delta_K} \int_{-\infty}^{\infty} \frac{dx'}{|x'|} \int_{-\infty}^{\infty} dk_y'' K(k_y'') \exp\left(-\frac{x'^2}{\Delta_x^2}\right) \\ &\times \left[S(k_y) - k_y'' \frac{\partial S(k_y)}{\partial k_y} + \frac{k_y''^2}{2} \frac{\partial^2 S(k_y)}{\partial k_y^2}\right].\end{aligned} \tag{25}$$

where

$$\begin{aligned}K(k_y'') =& (2\rho_i^4 k_x^2 k_y^2) G(b,b) \exp\left[-\left(k_y'' \frac{\partial \omega_{\vec{k}}}{\partial k_y}\right)^2 \frac{1}{2s^2\omega_{*i}} \frac{\rho_i^2}{x'^2}\right] \\ &\times \left\{-k_y'' v_D \left[\left(\frac{1}{2} + \frac{G'(b,b)}{G(b,b)}\right)\eta_i - 1\right] - \left(k_y'' \frac{\partial \omega_{\vec{k}}}{\partial k_y}\right)^3 \frac{\eta_i}{2} \frac{v_D}{s^2\omega_{*i}} \frac{\rho_i^2}{x'^2} + k_y'' \frac{\partial \omega_{\vec{k}}}{\partial k_y}\right\}\end{aligned}$$

It is easy to show that $\Delta_K \simeq \left(\frac{\partial \omega_{\vec{k}}}{\partial k_y} \frac{1}{\sqrt{2} s \omega_{*i}} \frac{\rho_i}{\Delta_x}\right)^{-3}$, and we estimate $\Delta_{SK} \simeq k_y^3$. The integration, first in $k_y''$ then in $x'$, and using $\omega_{\vec{k}} \ll \omega_{*i}$, produces:

$$\gamma_{\vec{k}}^c \simeq \left(\frac{\pi}{2}\right)^{3/2} \frac{r\hat{s}}{q\rho_i} \frac{\rho_i^4 \Omega_i L_s}{(1+1/\tau)} \frac{\omega_{*i}}{\omega_{\vec{k}}} k_x^2 k_y^4 \Gamma_0(b) G(b,b) \left[\left(2 + \frac{G'(b,b)}{G(b,b)}\right)\eta_i - 1\right] \frac{\partial S}{\partial |k_y|}. \tag{26}$$

With $S(k_y)$ no longer appearing under an integral sign, the wave kinetic equation has the more tractable form of:

$$\frac{\partial S}{\partial t} - V_{k_y} S \frac{\partial S}{\partial |k_y|} = \gamma_{\vec{k}}^l S, \tag{27}$$

where $V_{k_y}$ is the coefficient of $\frac{\partial S}{\partial |k_y|}$ in Eq. (26). Equation (27) has the form of a transport equation in $k_y$ space, with the linear growth (damping) playing the role of a source (sink) term, and the Compton scattering playing the role of convection. The fact that $V_{k_y}$ is positive definite implies that the transport of spectral energy scatters to lower $|k_y|$.

It is a simple matter to solve Eq. (27) for the saturated state ($\partial/\partial t \to 0$). This yields (for $k_y > 0$, with the other half following from symmetry):

$$\begin{aligned} S(k_y) &= -\int_{k_0}^{k_y} dk_y' \frac{\gamma_{\vec{k}'}^l}{V_{\vec{k}_y'}} \\ &= -\int_{k_0}^{k_y} dk_y' \rho_i \frac{4}{\pi^{3/2}} \frac{q\rho_i}{r\hat{s}} (1+1/\tau) \left(\frac{\rho_i}{L_s}\right)^2 \frac{(\Delta_x/\rho_i)}{(\rho_i k_y')^3 (\rho_i k_x')^2} \frac{\omega_{\vec{k}'}}{\omega_{*i}'}, \\ &\times \frac{1}{\Gamma_0(b')G(b',b')} \frac{1}{[(2+G'/G)\eta_i - 1]} \frac{\eta_i - \eta_c}{\eta_i \eta_c} \end{aligned} \tag{28}$$

where $k_0$ is the maximum unstable $k_y$ ($\to \infty$ for $\eta_i \geq 1$), and we have applied the boundary condition that $\lim_{k_y \to \infty} S(k_y) = 0$. This integral is straightforward but algebraicly tedious. To the accuracy of this theory, a simple estimate suffices. The most important $k_y$ dependence of the integrand comes from $\eta_i - \eta_c(b)$, which determines the sign. The essential features of $\eta_c$ (asymptotics, threshold, etc.) are retained by the approximation:

$$\frac{1}{\eta_c} \simeq \left\{ \begin{array}{ll} \frac{1}{2} + \left(\frac{1}{\eta_{th}} - \frac{1}{2}\right) b & b < 1 \\ 1 + \left(\frac{1}{\eta_{th}} - 1\right) \frac{1}{b} & b \geq 1 \end{array} \right\},$$

where $\eta_{th} = 0.95$ is the minimum of $\eta_c(b)$, attained for $b \simeq 1$. Also important is the $k_y$ dependence coming from the terms which vary as $k_y$ to a power. Noting that for $b \gtrsim 1$ it is appropriate to expand for $\Gamma_0$ and $G$ asymptotically, so that we obtain:

$$\frac{(\Delta_x/\rho_i)}{(\rho_i k_y)^3 (\rho_i k_x)^2} \frac{\omega_{\vec{k}}}{\omega_{*i}} \frac{1}{\Gamma_0(b)G(b,b)} \simeq \frac{2\pi(1+1/\tau)}{\eta_i} \left(\frac{L_n}{L_s}\right)^2 \left(\frac{\Delta_x}{\rho_i}\right)^3 \frac{1}{b},$$

where we have taken $k_x \simeq k_y$, $\Gamma_0(b) \simeq (2\pi b)^{-1/2}$ (Ref. 20), and $G(b,b) \propto b^{-1}$ is easily shown. If we use $\Delta_x$ as given by Eq. (13), then asymptotically we have $\Delta_x^2 \simeq 1/2b$. For all the rest of the $k_y$ dependence, substituting $(k_y\rho_i)_{\rm rms} \simeq 1$ suffices. We now perform the integral in Eq. (28), obtaining

$$S(k_y) \simeq \sqrt{\frac{2}{\pi}} \left(\frac{q\rho_i}{r\hat{s}}\right) \frac{(1+1/\tau)^2}{\eta_i^2} \left(\frac{L_n}{L_s}\right)^2 \left(\frac{\rho_i}{L_s}\right)^2 I(b). \tag{29}$$

Here, $I(b)$ is a spectral intensity function, defined as follows. If $\eta_i \leq \eta_{th} = 0.95$, then $I(b) = 0$. If $\eta_i > \eta_{th}$ (within the limits of validity of the theory), then

$$I(b) = \left\{ \begin{array}{ll} \frac{1}{3}\left(1 - \frac{1}{\eta_i}\right)\left(\frac{1}{b^{3/2}} - \frac{1}{b_0^{3/2}}\right) + \frac{1}{5}\left(\frac{1}{\eta_{th}} - 1\right)\left(\frac{1}{b^{5/2}} - \frac{1}{b_0^{5/2}}\right) & b \geq 1 \\ I(1) + \frac{1}{3}\left(\frac{1}{2} - \frac{1}{\eta_i}\right)\left(\frac{1}{b^{3/2}} - 1\right) + \left(\frac{1}{\eta_{th}} - \frac{1}{2}\right)\left(\frac{1}{b^{1/2}} - 1\right) & b < 1 \\ 0 & \text{if } I(b) < 0 \\ & \text{otherwise} \end{array} \right\}$$

The parameter $b_0$ (*i.e.*, $k_0$) is the maximum unstable b (given the above approximation for $\eta_c$)

$$b_0 = \left\{ \begin{array}{ll} \text{undefined} & \eta_i < \eta_{th} \\ \frac{1-\eta_{th}}{1-\eta_i} & \eta_{th} \leq \eta_i < 1 \\ \infty & 1 \leq \eta_i \end{array} \right\}$$

Figure 2 shows $I(b)$ for the cases $b_0 < \infty$ and $b_0 \to \infty$. In both cases, the spectrum is concentrated about the region $b \simeq 1$.

The first thing to notice about the spectrum is that the amplitude, $S \sim \frac{L_n^2}{L_s^2}\frac{\rho_i^2}{L_s^2}$ (i. e., the coefficient of $I(b)$ in Eq. (29), less the toroidal mode density terms $\frac{q\rho_i}{r\hat{s}}$), is extremely low in comparison to the saturation level in the fluid regime[1] (where $S \sim \frac{\rho_i^2}{L_s^2}$), even when the diminished linear growth rate due to the threshold is taken into consideration. Thus, Compton scattering seems to be much more effective than triad resonances at transferring energy away from unstable modes, thereby holding the turbulent fluctuations to a much lower level. However, as $\eta_i$ rises from the threshold level to the fluid level, $\gamma$ becomes greater than $\omega$, and the resonant part of $Z(\zeta)$ becomes zero.[21] Thus, in the fluid regime Compton scattering vanishes, allowing triad resonances to become the saturation mechanism, and $S(k_y)$ rises to the level of Ref. 1.

It is useful to devise a rule of thumb for estimating saturation levels from Compton scattering, although nothing as simple and broadly applicable as the mixing length estimate seems possible. From inspection of Eq. (23), it is easy to see that the the Compton scattering rate may be estimated by

$$\gamma_{\vec{k}}^{c} \sim \frac{\Omega_i^2}{\omega}(\rho_i k_\perp)^4 \frac{\omega_{*i}}{k_\| v_i}\left(\frac{e\tilde{\phi}}{T}\right)^2 ,$$

for the present ordering. Balancing $\gamma_{\vec{k}}^{c}$ with the linear growth gives the estimate

$$\sum_{\vec{k}}\left(\frac{e\tilde{\phi}_{\vec{k}}}{T}\right)^2 \sim \frac{\gamma\omega}{\omega_{*i}^2}\frac{\Delta_x/\rho_i}{(k_\perp\rho_i)^4}\frac{\rho_i^2}{L_n L_s}. \tag{30}$$

Using $\gamma$ and $\omega$ from Eqs. (12) and (14), and $\Delta_x \sim k_\perp^{-1} \sim \rho_i$, then Eq. (30) recovers the spectral amplitude of Eq. (29). This estimate is limited to the present ordering, although one might hope to derive a more general form from balancing the $\epsilon''$ and $\epsilon^{(3)}$ terms in Eq. (21).

Considering the approximations leading up to Eq. (29), it is essential to justify the main features of our nonlinear theory on physical grounds. First, the amplitude of the spectrum is roughly the same as given by scaling-type estimates[19] based on Eqs. (22) and (23), with $(k_y\rho_i)_{\rm rms} \simeq 1$, as above. Thus, it appears that the approximations after this equation did not lead to any miscalculation in the basic amplitude of $\tilde{\phi}$. Second, the result that energy scatters to lower $k_y$ is the usual result for ion Compton scattering, *e.g.* as in the case of drift wave turbulence.[17,22] Furthermore, it is reasonable to expect that retaining nonlocal interaction in $k_y$ space (neglected when $S(k_y')$ is expanded) would only further enhance this flow from the high $k_y$ source to the low $k_y$ sink. Third, our theory suggests that the spectral energy sink occurs for the $k_y\rho_i \simeq 1$, weakly stable ($|\gamma| < |\omega|$) modes. One might ask if the strongly stable $k_y\rho_i \ll 1$ modes might provide a more effective energy sink, and do not appear in our spectrum only as an artifact of neglecting long range interaction in $k_y$-space. To answer this point, we note that Compton scattering requires that both $S(k_y)$ and $S(k_y')$ be nonzero for transfer from $\vec{k}$ to $\vec{k}'$, while at the same time the strongly stable modes cannot be sufficiently destabilized by nonlinear coupling with weakly unstable modes. Thus, one expects that the weakly stablized modes (which *can* be nonlinearly destabilized to finite amplitude) should provide the dominant energy sink, as this theory shows. Finally, the nonlinear calculation indicates a spectrum that decays as $1/k_y^3$ as $k_y \to \infty$, although the linear theory suggests instability in this limit. This may be due to the fact that Compton scattering produces nonlinear stability at low amplitudes in this limit, but in any event, consideration of ion collisions or electron dissipation would stabilize the high $k_y$ modes, and so a vanishing spectrum is physically correct.

## V. Transport

Having obtained the saturated spectrum, we next apply this knowledge to finding the saturation level of ion thermal conductivity, $\chi_i$, due to turbulent $\vec{E} \times \vec{B}$ convection. Other transport coefficients are of secondary interest here, since it is the balance of heating and $\chi_i$ that determines $\eta_i$, and thus the relevance of this threshold regime to experiments. Turbulent transport is described by the guiding center Vlasov equation averaged over fast fluctuations:

$$\frac{\partial \langle F \rangle}{\partial t} + \mathrm{non-turbulent\ terms} = \frac{c}{B}\left\langle \tilde{\vec{E}} \times \hat{b} \cdot \nabla \tilde{f} \right\rangle, \tag{31}$$

where $F = \langle F \rangle + \tilde{f}$ is the phase space distribution function, and $\langle \ldots \rangle$ represents an average over fast fluctuations. The right hand side of this equation can be written as the divergence of a "flux", $-\nabla_x \Gamma_x(\vec{v})$, where

$$\Gamma_x(\vec{v}) = \frac{c}{B} \sum_{\vec{k}} -ik_y J_0\left(\frac{k_\perp v_\perp}{\Omega_i}\right) \left\langle \tilde{\phi}_{\vec{k}} \tilde{h}_{-\vec{k}} \right\rangle .$$

Treating $\Gamma_x(\vec{v})$ similarly to the nonlinearity in the gyrokinetic equation yields, after some work,

$$\Gamma_x(\vec{v}) = Im\sum_{\vec{k}} k_y\Big\{ -\mu^{(1)}_{\vec{k}}(\vec{v})\left|\tilde{\phi}_{\vec{k}}\right|^2 + \sum_{\substack{\vec{k}'+\vec{k}''=\vec{k}\\ \omega'+\omega''=\omega}} \frac{2\mu^{(2)}_{\vec{k}',\vec{k}''}(\vec{v})\epsilon^{(2)}_{-\vec{k}',-\vec{k}''}}{\epsilon^{(1)}_{\vec{k}'+\vec{k}''}}\left|\tilde{\phi}_{\vec{k}'}\right|^2\left|\tilde{\phi}_{\vec{k}''}\right|^2$$

$$+ \sum_{\substack{\vec{k}'+\vec{k}''=\vec{k}\\ \omega'+\omega''=\omega}} \frac{4\mu^{(2)}_{\vec{k}',\vec{k}''}(\vec{v})\epsilon^{(2)}_{\vec{k},-\vec{k}'}}{\epsilon^{(1)}_{\vec{k}''}}\left|\tilde{\phi}_{\vec{k}'}\right|^2\left|\tilde{\phi}_{\vec{k}}\right|^2$$

$$- \sum_{\vec{k}'+\vec{k}''=\vec{k}} \mu^{(3)}_{\vec{k}',-\vec{k}',\vec{k}}(\vec{v})\left|\tilde{\phi}_{\vec{k}'}\right|^2\left|\tilde{\phi}_{\vec{k}}\right|^2\Big\}, \tag{32}$$

where the $\mu^{(n)}(\vec{v})$ are equal to the corresponding $\epsilon^{(n)}$ without the velocity space integration, and the redundant arguments $\omega$ have been omitted from both of these. The similarity of the Eq. (32) and the right hand side of Eq. (21) is obvious. The $\vec{v}$-moments of $\Gamma_x(\vec{v})$ give the fluxes of the fluid quantities. The particle flux, $\int d^3v\Gamma_x(\vec{v})$, is proportional to the right hand side of the wave kinetic equation, which vanishes at saturation. A phase shift between $\tilde{n}_e$ and $\tilde{\phi}$ (here, adiabatic) would be needed to model particle flux. The ion thermal flux, $q_i = \int d^3v\frac{mv^2}{2}\Gamma_x(\vec{v})$, is a more involved calculation. For the same reasons as in the wave kinetic equation, we retain only the quasilinear and Compton pieces of $\Gamma_x(\vec{v})$ (the first and last terms in Eq. (32), respectively), and obtain (after extensive calculation)

$$\begin{aligned} q_i = &-2\sqrt{\pi}v_i n_0 T_i(1+1/\tau)\frac{r\hat{s}}{q\rho_i}\frac{L_n}{L_s} \\ &\times\int_{-\infty}^{\infty} dk_y\rho_i k_y^2\Delta_x^2\frac{\omega_{*i}}{\omega_{\vec{k}}}(1-2b+b^2+b\frac{\Gamma_1}{\Gamma_0}-b^2\frac{\Gamma_1^2}{\Gamma_0^2})S(k_y), \end{aligned} \tag{33}$$

where we have neglected terms of order $\gamma/\omega$ or less. Inserting the spectrum from Eq. (29) and expanding $\Gamma_n(b)$ for $b \gtrsim 1$, we find the ion thermal conductivity:

$$\begin{aligned} \chi_i &= -q_i\Big/n_0\left(\frac{dT_0}{dx}\right) \\ &\simeq N_{th}\frac{(1+1/\tau)^2}{2\sqrt{\pi}}\left(\frac{L_T}{L_s}\right)^2\frac{\rho_i^2 v_i}{L_s}, \end{aligned} \tag{34}$$

where $N_{th}$ is the $k_y$ integrated spectrum, and contains the cutoff of $\chi_i$ at threshold:

$$\begin{aligned} N_{th} &= \int_0^{\infty} db I(b) \\ &= \left(1-\frac{1}{\eta_i}\right)\left(1-\frac{1}{b_0^{1/2}}\right)+\frac{1}{3}\frac{1}{(\eta_{th}-1)}\left(1-\frac{1}{b_0^{3/2}}\right)\left(\frac{1}{\eta_{th}}-\frac{1}{\eta_i}\right)\sqrt{2I(1)}, \end{aligned} \tag{35}$$

where $b_0$ and $I(1)$ are defined in Section IV. The integrated spectrum, $N_{th}$ is a function of $\eta_i$ only, and is plotted in Figure 3. A simple calculation shows that $N_{th} \propto (\eta_i - \eta_{th})^2$ just above threshold, so that the onset of turbulence is gradual as $\eta_i$ increases above its threshold.

This calculation is valid in the regime $\eta_{th} = 0.95 \leq \eta_i \leq \eta_{th} + (1 + 1/\tau)L_n/L_s$, and $L_n/L_s \ll 1$. When $\eta_i$ rises above this regime, $\gamma \ll \omega$ no longer holds, and Compton scattering decreases, and is replaced by mode coupling, enhanced by frequency broadening effects. Accompanying this transition is a rise in the saturated level of fluctuation, and $\chi_i$ increases to the level predicted by the strong turbulence theory of Ref. 1 (valid when $\eta_i \gg \eta_{th}$).

It is useful to note that the usual $\chi_i \simeq \gamma^l \Delta_x^2$ estimate predicts a $\chi_i$ that is too high by a factor of about $(L_s/L_n)^2$, and therefore doesn't apply to the present weak turbulence case. A more appropriate estimate, based on the quasilinear piece of Eq. (32), is

$$\chi_i \sim L_T k_y \Delta_x^2 \Omega_i \frac{1}{\eta_i - \eta_{th}} \frac{\gamma}{\omega} \left( \frac{e\tilde{\phi}}{T_i} \right)^2 ,$$

where the term $\eta_i - \eta_{th}$ cancels the corresponding term in $\gamma$ (reflecting the fact that $\chi_i$ comes from the $v^2$ moment of $\mu(\vec{v})$, and not the $v^0$ moment, as does $\gamma$). Using the estimate of $e\tilde{\phi}/T_i$ from Eq. (30), we get

$$\chi_i \sim \frac{\gamma^2}{\omega_{*_i}^2} \frac{1}{(k_\perp \rho_i)^6} \frac{\rho_i}{L_s} \Omega_i \rho_i^2 .$$

This estimate follows from the orderings of the $\eta_i \sim \eta_{th}$ case, and hence is not as broadly applicable as the $\gamma/k_\perp^2$ estimate from strong turbulence.

## VI. Discussion

This paper has explored the behaviour of the sheared slab $\eta_i$ mode near the threshold of instability, applicable to the regime $\eta_{th} \leq \eta_i \lesssim \eta_{th} + (1 + 1/\tau)L_n/L_s$. Linear stability is determined by the balance of the ion temperature gradient drive and ion Landau damping. The unstable modes have $k_\perp \rho_i \simeq 1$ and $\gamma < \omega$ when $\eta_i$ is in this regime. Thus, a weak turbulence expansion is applicable. Nonlinearly, the saturation amplitude is determined by the balance of linear growth and ion Compton scattering. This results in a spectrum peaked about $k_\perp \rho_i \simeq 1$ and with an amplitude that is of order $(L_n/L_s)^2$ relative to naïve extrapolation from the fluid regime. The resulting ion thermal conductivity, $\chi_i$, is at a similarly low level. In experimental situations, this low level of $\chi_i$ near threshold is probably obscured by competing mechanisms such as neoclassical transport.

The significance of this work is that it gives insight into the regime of $\eta_i$ turbulence that is applicable to experiments. Since $\chi_i$ in the threshold regime, is extremely low, we expect that the strong heating in modern tokamaks should easily drive $\eta_i$ beyond this. For $\eta_i \gg \eta_{th}$, fluid theory predicts extremely large $\chi_i$, driving $\eta_i$ down toward the threshold, even in the presence of strong ion heating.[10] Thus, it appears that the balance of ion heating and ion thermal conductivity results in an $\eta_i$ in between these two extremes. The linear theory of this study indicates that there is an intermediate regime that differs from either extreme. The linear modes of this middle regime are characterized by a fluid-like interior, ion Landau damping at the edges, and $\gamma \gtrsim \omega$ (prohibiting a weak turbulence expansion). Modes with $l > 0$ become progressively destabilized in this regime, with their growth rate quickly surpassing that of the $l = 0$ mode. With these kinds of complications, developing a satisfactory analytical theory of this intermediate regime is quite a challenge. Short of such an analysis, one might assume on physical grounds that so long as linear ion resonances are important, then nonlinear ion resonances are also present, and the associated nonlinear Landau damping will maintain fluctuations at the low level indicated by this study. In this case, then large $\chi_i$ will occur only in the fluid regime, where resonances are negligible. Thus, the fluid predictions should determine the $\eta_i$ transport relevant to experiments.

Of experimental interest, these results suggest that a steeper ion temperature profile will accompany effects that increase the weak/strong turbulence transition point, $\eta_{\rm th}^{\rm W} \simeq$

$\eta_{\rm th} + (1 + T_i/T_e)L_n/L_s$. This might explain the improved confinement with increased $T_i/T_e$ as observed on TFTR,[23] and with increased current ($\propto 1/L_s$) on many tokamaks.[24] Also, the broadening of the weak turbulence regime with increased $L_n$ might be connected with the observation that flat density profiles ($L_n \to \infty$) do not seem to worsen H mode confinement (even though a purely fluid $\eta_i$-mode theory[25] indicates degraded $\chi_i$. Of course, a reliable estimate of whether these effects are strong enough to influence observations would require use of a transport code that models $\chi_i$ in both the strong and weak turbulence regimes.

The results of this paper suggest several possible directions for further study. Numerical solution of the integral equations (both linear and nonlinear) would be useful as a check of the analytical theory. Additional effects such as toroidal coupling[26] or trapped particles[27] could greatly alter the characteristics of the threshold regime, perhaps leading to more significant transport. Also, exploration of the regime that exists between the threshold and fluid regimes is clearly interesting. Finally, a weak turbulence analysis for flat density profiles would resolve whether the effects found in this paper can account $\eta_i$ transport during H modes.

### Acknowledgements

The authors would like to thank M. N. Rosenbluth, P. W. Terry, and T. S. Hahm, for useful conversations, and M. E. Glinsky for discussing the possibility of numerical solution of the integral equation.

This work has been supported by the United States Department of Energy under Contract No. DE-FG05-80ET-53088, University of Texas, Austin, and under Grant No. DE-FG03-88ER-53275, University of California at San Diego.

## Appendix A: Stability of Higher Radial Eigenmodes

In Section III, we obtained the growth rate of the $l = 0$ mode by averaging the local growth rate over the normal mode. Here, we apply this technique to the $l > 0$ modes. These are broader, and experience more Landau damping away from the rational surface; this underlies the result that the stability threshold increases sharply with $l$.

Averaging the local growth rate in Eq. (9), with $k_\| = k_y x/L_s$, over the modes given by Eq. (11), and using the mode width given by Eq. (13), we find

$$\gamma_{k_y,l} = \sqrt{2}\,\omega_{*i} s(2l+1)\frac{\Delta_x^{l=0}}{\rho_i}\left[I_l^{[3/2]}\frac{1}{\eta_i}\left(\frac{\eta_i}{\eta_c}-1\right) - \frac{3}{2}I_l^{[5/2]}(2l+1)^2\left(\frac{\Delta_x^{l=0}}{\rho_i}\right)^2\frac{p(p-1)}{\eta_i^2}s^2\right] \tag{A1}$$

where

$$I_l^{[r]} = \frac{\sqrt{\pi}\,2^l\,F(-l,-l;-l+r;\frac{1}{2})}{2\,l!\,\Gamma(-l+r)}, \qquad p = \frac{1+1/\tau}{\Gamma_0},$$

$$\Delta_x^{l=0} = (1-\Gamma_1/\Gamma_0)^{1/2}\rho_i, \qquad s = \frac{L_n}{L_s}, \qquad \Gamma_n = e^{-b}I_n(b),$$

$F$ is a hypergeometric function, and $\Gamma$ is the gamma function (not to be confused with $\Gamma_n$). The first several $I_l^{[r]}$ are listed in Table 1. In deriving Eq. (A1), we have assumed that $2l+1 < \eta_i/s$, so that the exponential in $\gamma_{\vec{k}}(k_\|)$ may be neglected relative to the exponential in Eq. (11). For $l = 0$, Eq. (A1) reduces to Eq. (14).

Setting $\gamma_{k_y,l}$ to zero and solving for the $\eta_i > 0$ branch yields the stability threshold for the higher radial eigenmodes

$$\eta_c^l = \eta_c\left[\tfrac{1}{2} + \left(\tfrac{1}{4} + C_l\frac{(1-\Gamma_1/\Gamma_0)p(p-1)}{\eta_c}s^2\right)^{1/2}\right], \tag{A2}$$

where $C_l = \frac{3}{2}(2l+1)^2 I_l^{[5/2]}/I_l^{[3/2]}$. The basic threshold, $\eta_c$, is modified by the term which varies as $C_l$. The modification is of order $s^2 \ll 1$, and is extremely small for the $l = 0$ mode; however, the coefficient is a rapidly increasing function of $l$, which raises the threshold significantly for $l > 0$ (see Table 1 and Fig. 4). This higher threshold agrees with the shooting code results of Ref. 13. They are also consistent with the kinetic shooting code result[16] that for weaker shear (*i.e.*, smaller $s$) a larger number of eigenmodes are unstable.

Once $\eta_i$ rises above the threshold for the higher $l$ modes, the growth rate increases rapidly, so that above the threshold regime these modes dominate the transport.[16] However, it should be noted that $\eta_i$ must be significantly greater than 1 for a large number of the higher $l$ modes to be in the fluid regime. This is unlikely in light of the strong thermal transport they cause. Thus, we can expect that at most, only the first few radial eigenmodes are relevant to tokamak regimes.

## Appendix B: Stability of Flat Density Modes

Here, we use the technique of Section III to calculate stability in the limit $1 \ll L_n/L_s \to \infty$ (formerly assumed small). This may be considered either as the limit of flat density, or as stabilization coming from increased shear. In this limit, the dielectric function of Eq. (5) becomes

$$\epsilon_{\vec{k}}(\omega) = 1 + 1/\tau - \frac{\omega_*^T}{\omega}\Gamma_0\zeta^2 + \frac{\omega_*^T}{\omega}\left(\frac{1}{\eta_c} - \zeta^2 + \frac{\omega}{\omega_*^T}\right)\Gamma_0\zeta Z(\zeta), \tag{B1}$$

where $\omega_*^T = k_y\rho_i^2\Omega_i/L_{T_i}$. Treated locally using the $\gamma = \frac{-\epsilon''}{(\partial\epsilon'/\partial\omega)}$ approximation as before, with $k_{\|}$, this yields

$$\gamma_{\vec{k}}(x) = \sqrt{2\pi}\omega_*^T\frac{L_T}{L_s}\frac{|x|}{\rho_i}\left[\frac{1}{\eta_c} - 2p(p-1)\left(\frac{L_T}{L_s}\right)^2\left(\frac{x}{\rho_i}\right)^2\right]\exp\left[-2\left(\frac{L_T}{L_s}\frac{x}{\rho_i}\right)^2\right]. \tag{B2}$$

Arguing as after Eq. (9) gives the result that only for $(L_s/L_T)^2 \to 0$ is $\gamma(x)$ stable for all $x$. Thus, locally there is instability for all values of $L_T$. However, from our quasi-local point of view, $\gamma(x)$ must be positive over a wide enough region to give a net positive energy input to the mode. The normal modes in this regime are described, as in the $L_n/L_s \ll 1$ theory, by Eqs. (11)-(13) (the first three terms of Eqs. (5) and (B1) are the same, and the rest are subdominant in both threshold regimes). Averaging $\gamma(x)$ over the $l = 0$ mode produces

$$\gamma_{\vec{k}} = \sqrt{2}\frac{L_T}{L_s}\omega_*^T\frac{\Delta_x}{(\rho_i^2 + (\Delta_x pL_T/L_s)^2)^{1/2}}\left[\frac{1}{\eta_c} - \frac{2p(p-1)}{\Delta_x^2/\rho_i^2}\frac{L_T^2}{L_s^2} - 2p^3(p-1)\frac{L_T^4}{L_s^4}\right]. \tag{B3}$$

This shows that the threshold for $\nabla T_i$ is given by

$$\left(\frac{L_s}{L_T}\right)_c^2 = \eta_c\frac{p(p-1)}{\Delta_x^2/\rho_i^2}\left[1 + \left(1 + \frac{2(\Delta_x/\rho_i)^4 p}{\eta_c(p-1)}\right)^{1/2}\right]. \tag{B4}$$

For $b = 0$, then $(L_s/L_T)_c$ is about $\sqrt{2(1+\tau)/\tau^2}$, and increases rapidly with $b$. Thus, it appears that modes with $b \ll 1$ are the most relevant to the flat density regime.

## Appendix C: Normalization of the Expanded Spectrum

This Appendix demonstrates that the step of expanding $S(k'_y)$ under the integral (as in going from Eq. (24) to Eq. (25)) must be accompanied by a normalization of the integral. Here, we show this when $S(k'_y)$ is a gaussian, and assume on intuitive grounds that this holds for more general shapes of $S$.

Letting $S(k') = e^{-k'^2/\Delta_S^2}$ and $K(k'') = k'' e^{-k''^2/\Delta_K^2}$ (which is the form of the kernel in Eq. (25)), then it is easy to show that the exact integral is

$$\int_{-\infty}^{\infty} S(k')K(k'')dk' = \frac{\Delta_S \Delta_K^3}{(\Delta_S^2 + \Delta_K^2}\sqrt{\pi}k \exp\left[-k^2/(\Delta_S^2 + \Delta_K^2)\right]. \tag{C1}$$

Now, if $S(k')$ is Taylor expanded about $k$, where $k = k' + k''$, then the integral is

$$\int_{-\infty}^{\infty} \left[S(k) - k''\frac{dS}{dk} + \frac{k''^2}{2}\frac{d^2S}{dk^2}\right] K(k'')dk' = \frac{\Delta_K^3}{\Delta_S^2}\sqrt{\pi}k \exp\left[-k^2/\Delta_S^2\right]. \tag{C2}$$

In the limit where $\Delta_K \ll \Delta_S$, for which such an expansion is fully consistent, then Eqs. (C1) and (C2) are the same. However, in our case, $\Delta_K \gg \Delta_S$, so that Eq. (C2) must be multiplied by $(\Delta_S/\Delta_K)^3 \exp\left[-k^2\left(\frac{\Delta_K^2 - \Delta_S^2}{\Delta_K^2\Delta_S^2}\right)\right]$ to agree with the correct answer. The exponential part of this normalization is of order 1 for modes in the spectrum (*i.e.*, those for which $k \lesssim \Delta_S$), as well as an artifact of the gaussian shape of $S$, so we ignore it. (In comparing this derivation with the normalization used in Section IV, one should keep in mind that the width of $k''K$ varies as $\Delta_K^3$, and the width of $SK$ varies as $\Delta_S^3$.)

## References


1. G. S. Lee and P. H. Diamond, Phys. Fluids **29**, 3291 (1986).
2. R. J. Groebner, W. W.Pfeiffer, F. P. Blau, and K. H. Burrell, Nuclear Fusion **26**, 543 (1986).
3. A. A. Galeev, V. N. Oraevskiĭ, and R. Z. Sagdeev, Sov. Phys. JETP **17**, 615 (1963).
4. M. Greenwald, D. Gwinn, S. Milora, J. Parker, R. Parker, and S. Wolfe *10th International Conference on Plasma Physics and Controlled Nuclear Fusion Research*, London (IAEA, Vienna, 1984), Vol. I, p. 45.
5. D. O. Overskei, C. J. Armentrout, J. F. Baur, F. P. Blau, G. Bramson, K. H. Burrell, R. P. Chase, J. C. DeBoo, S. Ejima, E. S. Fairbanks, R. Groebner, C. L. Hsieh, G. L. Jahns, C. L. Kahn, D. H. Kellman, D. Knowles, J. Lieber, J. M. Lohr, N. Ohyabu, T. W. Petrie, L. C. Rottler, D. P. Schissel, R. P. Seraydarian, J. R. Smith, R. T. Snyder, R. D. Stambaugh, R. E. Stockdale, H. St. John, E. J. Strait, C. S. Tucker, D. Vaslow, S. S. Wojtowicz, and S. K. Wong, in *Proceedings of the 4th International Symposium on Heating in Toroidal Plasmas* (International School of Plasma Physics, Varenna, 1984), p. 21.
6. D. L. Brower, W. A. Peebles, S. K. Kim, N. C. Luhmann Jr.,W. M. Tang, and P. E. Phillips, Phys. Rev. Lett. **59**, 49 (1987).
7. N. Mattor and P. H. Diamond, Phys. Fluids **31**, 1180 (1988).
8. R. J. Fonck, Bull. Am. Phys. Soc. **32**, 1846 (1987)
9. K. H. Burrell, R. J. Groebner, H. St. John, and R. P. Seraydarian, Nucl. Fusion **28**, 3 (1988).
10. R. J. Goldston, Y. Takase, D. C. McCune, M. G. Bell, M. Bitter, C. E. Bush, P. H. Diamond, P. C. Efthimion, E. D. Fredrickson, B. Grek, H. Hendel, K. W. Hill, D. W. Johnson, D. Mansfield, K. McGuire, E. Nieschmidt, H. Park, M. H. Redi, J. Schivell, S. Sesnic, and G. Taylor, in *14th European Conference on Controlled Fusion and Plasma Physics* (European Physical Society, Budapest, 1987), p. 140.
11. B. B. Kadomtsev and O. P. Pogutse in *Reviews of Plasma Physics* (Leontovitch, M. A., ed.), Vol. 5, pg. 249 (Consultants Bureau, New York, 1970).
12. T. Antonsen, B. Coppi, and R. Englade, Nucl. Fusion **19** 641 (1979).

13. R. E. Waltz, W. Pfeiffer, and R. R. Dominguez, Nucl. Fusion **20**, 43 (1980).

14. F. Romanelli, submitted for publication in Phys. Fluids.

15. E. A. Frieman and Liu Chen, Phys. Fluids **25**, 502 (1982).

16. P. W. Terry, J. N. Leboeuf, P. H. Diamond, D. R. Thayer, and G. S. Lee, accepted for publication in Phys. Fluids.

17. R. Z. Sagdeev and A. A. Galeev, **Nonlinear Plasma Theory**, edited by T. M. O'Neil and D. L. Book (Benjamin, New York, 1969).

18. B. Coppi, M. N. Rosenbluth, and R. Z. Sagdeev, Phys. Fluids **10**, 582 (1967).

19. N. Mattor and P. H. Diamond, *Proceedings of the 1988 Sherwood Controlled Theory Conference* (Oak Ridge National Laboratory, Oak Ridge, 1988) p. 2C09.

20. F. W. J. Olver, Chapter 9 of **Handbook of Mathematical Functions**, edited by M. A. Abramowitz and I. A. Stegun (National Bureau of Standards Applied Mathematics Series 55, 1972).

21. B. Fried and S. Conte, **The Plasma Dispersion Function** (Academic Press, New York, 1961).

22. P. H. Diamond and M. N. Rosenbluth, Phys. Fluids **24**, 1641 (1981).

23. M. C Zarnstorff, M. G. Bell, M. Bitter, C. Bush, R. J. Fonck, R. J. Goldston, B. Grek, K. W. Hill, R. B. Howell, H. Hsuan, K. P. Jaehnig, D. W. Johnson, R. Knize, D. Mansfield, H. Park, A. Ramsey, J. Schivell, and G. Taylor, Bull. Am. Phys. Soc.**33**, 1882 (1988).

24. Stanley M. Kaye, Phys. Fluids **28**, 2327 (1985).

25. N. Mattor and P. H. Diamond (in preparation).

26. P. N. Guzdar, Liu Chen, W. M. Tang, and P. H. Rutherford, Phys. Fluids **26**, 673 (1983).

27. M. Tagger, G. Laval, and R. Pellat Nucl. Fusion **17**, 109.

| $l$ | $I_l^{[3/2]}$ | $I_l^{[5/2]}$ | $C_l$ |
|---|---|---|---|
| 0 | 1 | 2/3 | 1 |
| 1 | 2 | 8/3 | 18 |
| 2 | 5/2 | 17/3 | 85 |
| 3 | 3 | 28/3 | 228.7 |
| 4 | 27/8 | 163/12 | 489 |
| 5 | 15/4 | 55/3 | 887.3 |
| 6 | 65/16 | 565/24 | 1469 |

**Table 1:** Functions used in Eqs. (A1) and (A2).

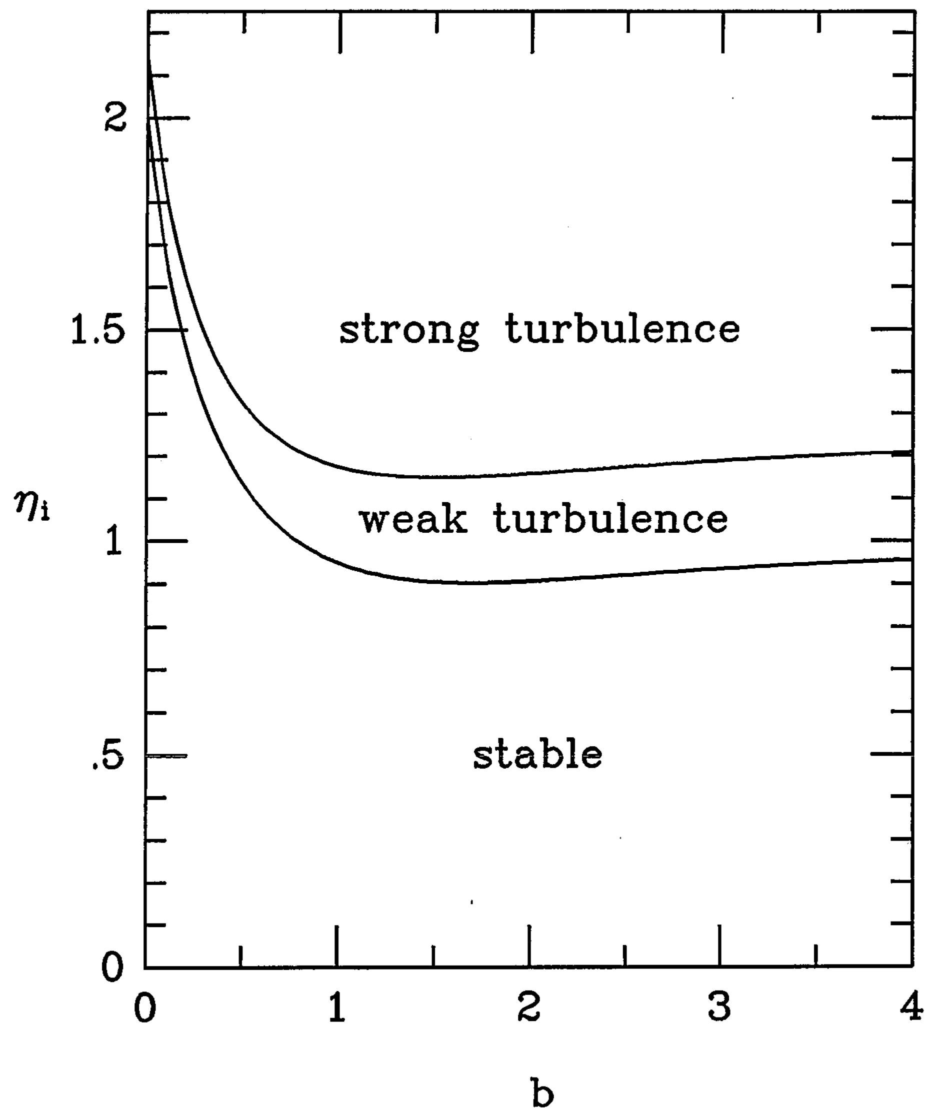


**FIGURE 1:** Stability threshold and weak turbulence regime, where $\gamma \ll \omega$, for $L_n/L_s = 0.1$, $\tau = 1$.

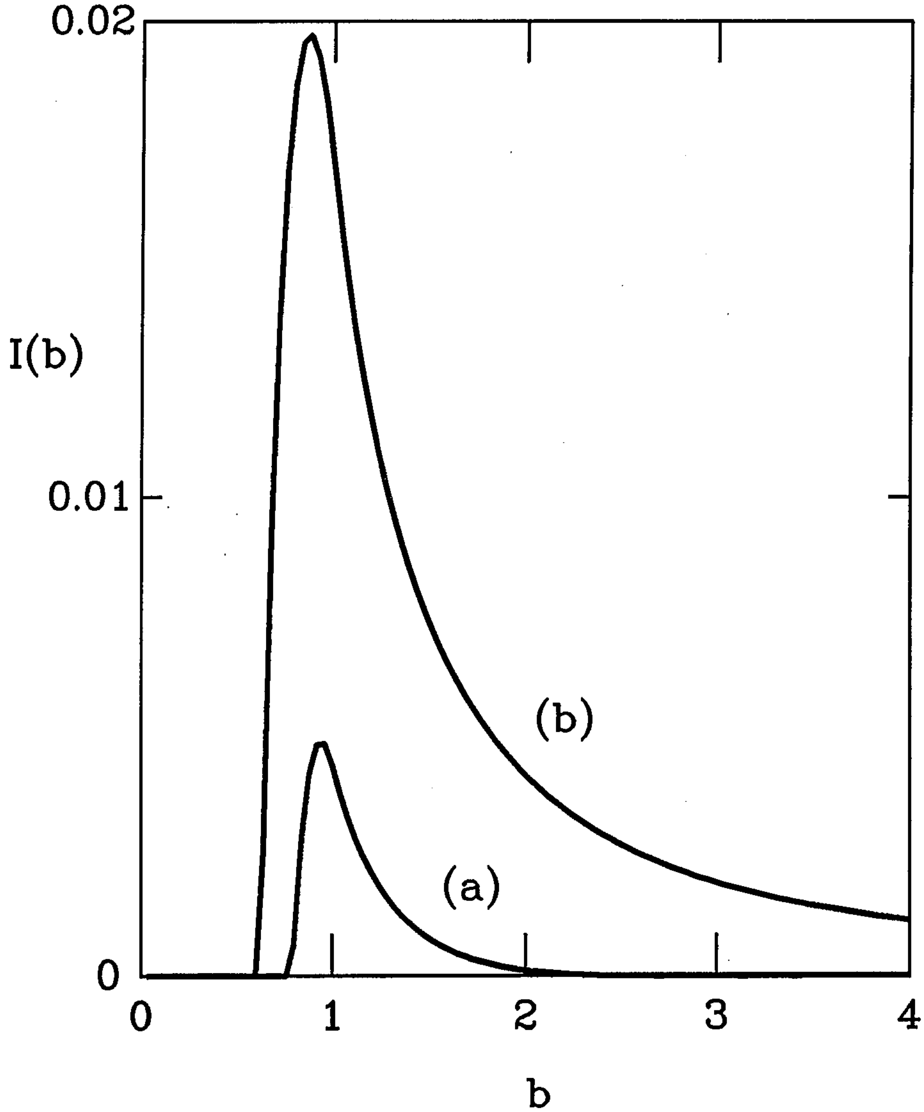


**FIGURE 2:** Form of wavenumber spectrum in Eq. (29) (a) for $\eta_i = .98$ and (b) for $\eta_i = 1.02$.

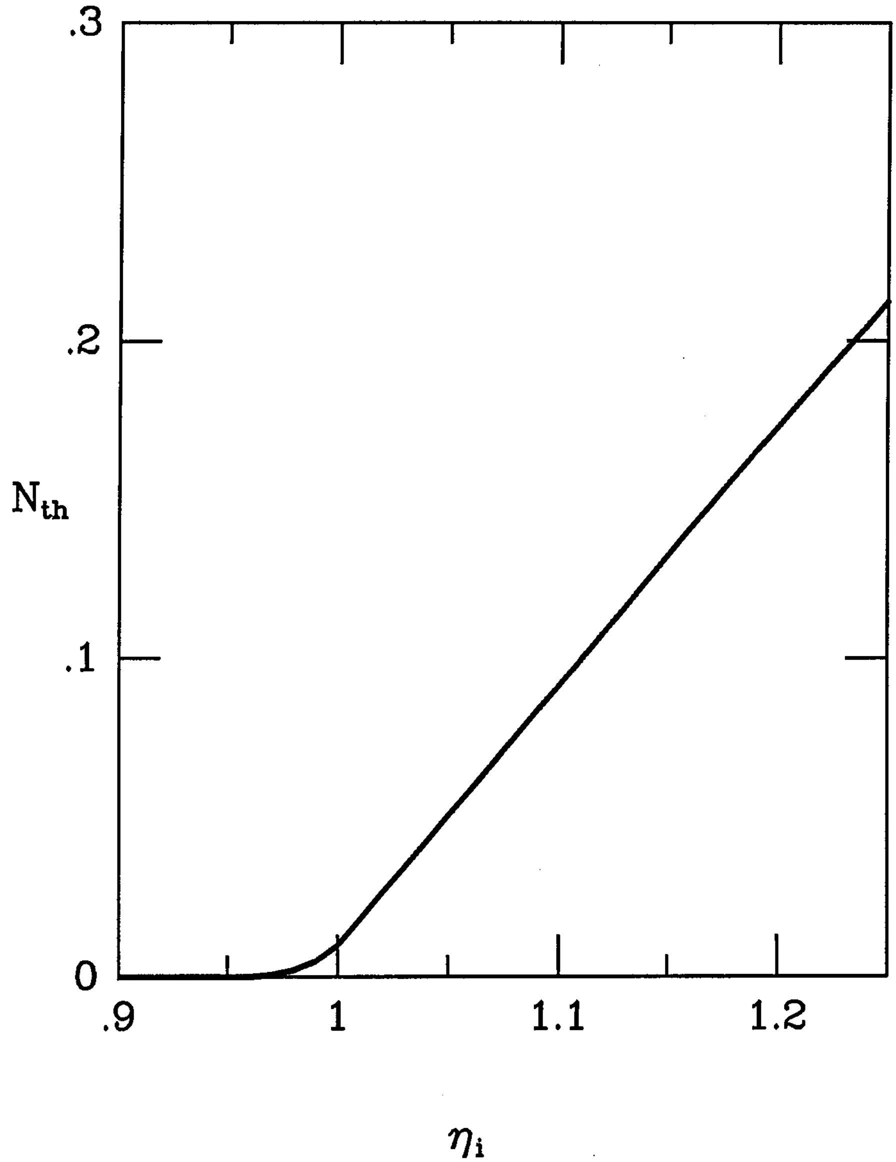


**FIGURE 3:** Integrated spectrum appearing in $\chi_i$, Eq. (33).

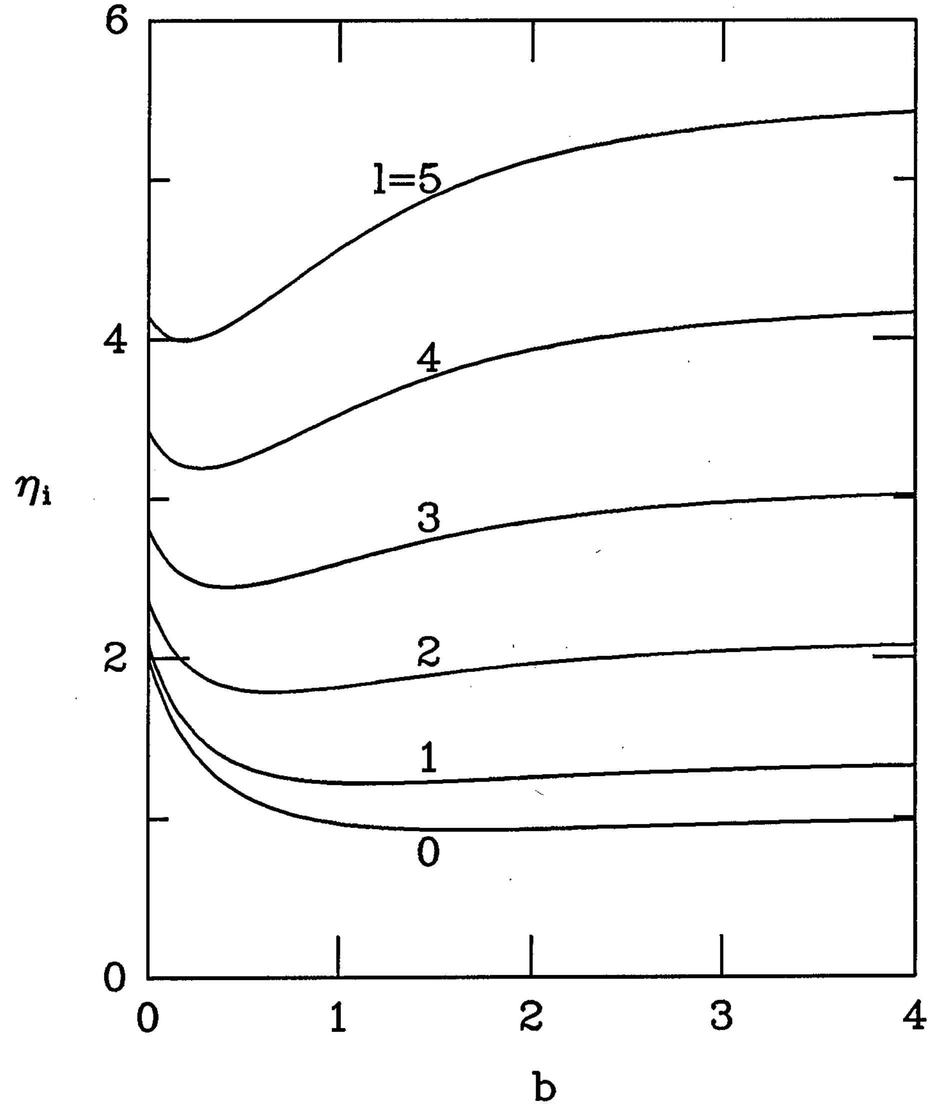


**FIGURE 4:** Stability threshold for higher radial eigenmodes, with $L_n/L_s = 0.05$ and $\tau = 1$.